2007

Oxidation Resistant Coatings on Microcelluar Carbon Foam using Simple Scalable Techniques

Dakshinamurthy Sharma Nagalingam
Wright State University

OXIDATION RESISTANT COATINGS ON MICROCELLUAR CARBON FOAM USING SIMPLE SCALABLE TECHNIQUES

A thesis submitted in partial fulfillment
of the requirements for the degree of
Master of Science in Engineering

By

DAKSHINAMURTHY SHARMA NAGALINGAM
Bachelor of Engineering, Osmania University, India, 2003.

2007
Wright State University

WRIGHT STATE UNIVERSITY

SCHOOL OF GRADUATE STUDIES

04/30/2007

I HEREBY RECOMMEND THAT THE THESIS PREPARED UNDER MY GUIDANCE BY DAKSHINAMURTHY SHARMA NAGALIGAM ENTITLED Oxidation Resistant Coatings on Microcellular Carbon Foam using Simple Scalable Techniques BE ACCEPTED IN PARTIAL FULFILLMENT OF THE REQUIREMENTS FOR THE DEGREE OF Master of Science in Engineering

_____

Sharmila M Mukhopadhyay, Ph.D.
Thesis Director

_____

George P G Huang, Ph.D.
Department Chair

Committee on
Final Examination

_____
Sharmila M Mukhopadhyay, Ph.D.

_____
Raghavan Srinivasan, Ph.D.

_____
Allen G Jackson, Ph.D.

_____
Joseph F Thomas, Jr., Ph.D.
Dean, School of Graduate Studies

ABSTRACT

Nagalingam, Dakshinamurthy Sharma M.S.Egr., Department of Mechanical and Materials Engineering, Wright State University. *Oxidation Protective Coatings on Microcellular Carbon Foam Using Simple Scalable Techniques*.

Carbon foam has many applications in the fields of thermal management, net-shape composites and electronic cooling due to its porous structure, low density, electrical and thermal conductivities. However it is prone to oxidation at high temperatures in air. Whereas some previous studies have reported oxidation protective coatings on other carbon structures such as graphite parts and fibers, there is very limited work on foam. Moreover, earlier methods have used vapor phase techniques such as Plasma Vapor Deposition (PVD) and Chemical Vapor Deposition (CVD). There is no known study involving such coatings using simple scalable liquid phase method. This thesis reports our results on such coatings obtained on carbon foam. Boron Nitride was chosen as the coating material. Several solvents and processes were investigated. Finally a two step process using PVP binder in alcohol-based solution is found to be most effective. Unlike other available methods this technique does not involve toxic precursors or by-products. This method is simple and can be obtained at atmospheric pressure. Different coating combinations using various particle sizes were applied and their surface morphologies were studied using SEM (Scanning Electron Microscopy) and FESEM (Field Emission Scanning Electron Spectroscopy). It was observed that coating formed using 1μ BN followed by 0.7μ size BN particles has the best performance so far. The surface chemistry of this coating was studied using X-ray Photo Spectroscopy (XPS) and found to be that of pure BN after heat treatment. This coating was tested on several grades of

aerospace foams having different porosities and cell sizes. The testing shows that this layer enhances the oxidation resistance of all foams to a certain extent. However it is most effective on the foams that have ridged ligaments compared to those having smooth ligaments. On carbon foams having high surface roughness this layer could suppress oxidation even at 800^{o}C and enhance the survivability by 333%. This coating approach therefore shows promise as a scalable, environmentally friendly way of inhibiting oxidation in porous carbon structures.

CONTENTS

2 EXPERIMENTAL PROCEDURES

3 RESULTS AND DISCUSSION

LIST OF FIGURES

LIST OF TABLES

ACKNOWLEDGEMENTS

First and Foremost, I would like to express my deep sense of gratitude to my advisor to Dr. Sharmila Mukhopadhyay for her excellent guidance and continuous support without which I wouldn't have come so far. I would like to acknowledge the National Science foundation, Air Force Research Laboratory and Ohio Board of Regents for funding my research work.

I would like to thank Dr A.G.Jackson and Dr Raghavan Srinivasan for being part of thesis committee and also giving me valuable feedback on my work. I would like to thank Greg Wilt for assisting me in the labs. I also thank my colleague Ian Barney for his invaluable suggestions that helped me a lot in drafting my thesis work. I thank other members of our research group Vamsee Chintamaneni, Anil Karumuri Dr. Raja Pulikollu, Dr. Jianhua Su, and Dr. Pratik Joshi for their helpful discussions on my research. My special thanks to my friends Manoj, Sandeep, Gnani, Rajani, Suman, Hemanth with whom I shared a wonderful journey at Wright State University.

I am indebted to my parents (Mr. Babu Rajasekhara Prasad, Mrs. Hymavathi Devi) and my brother (Anand) for love and affection throughout my life. They are source of inspiration during challenging moments of my life.

Finally, I would also like to thank all my friends and well-wishers for helping me in one way or other during course of my research.

This work is dedicated to

My grandmother Mrs. Satyavati Devi

1 INTRODUCTION

1.1 History of Surface Engineering

The word engineering is derived from the French word s'ingenier meaning study or design. The term is used in a broad sense as the application of science to various fields like chemical, processing, mechanical and materials science engineering. The term materials science was coined in early 60's to denote a combined scientific discipline that investigates material structure, improvement, production and other related issues. The branch of material science that deals with enhancement or modification of surface properties was later known as surface engineering. Historically, thermal energy was used as a primary source of energy for surface modification. It is believed that in Asia, forging was used as early as 7000BC [1]. References are made to surface treatments in Homer's Odyssey and other Greek mythologies [4]. A 4^{th} century forged iron column in Delhi is a classical example of extraction and processing techniques that were used in those days [2]. Recently, traces of cementite nano wires were found in 400 year old historic Damascus steel made from Indian iron cakes [78]. French scientist Reaumur in his work "Magnum opus" was the first one to investigate surface treatments from scientific point of view [4]. Faraday's laws revolutionized the surface science by the use of electrical energy (like electro-plating) unlike conventional thermal energy [3]. Today new techniques are in use involving surface modification at nano scales.

1.2 Concept of Surface Engineering

The surface can be loosely defined as the edge or boundary of a material from which most changes in the material start [17]. Surface engineering is the concept of tailoring the outside of a material to accomplish surface properties that suit the requirement. It is especially useful when surface related phenomena weaken the structures. Traditional methods like quench hardening, nitriding and carbonizing as well modern approaches that make use of electrical, chemical and plasma energy contribute to surface modification. Surface engineering deals not only with designing and forming surface layers, but also with investigating the surface performance [fig (1.1)]. By using surface modification techniques the surface properties were enhanced as per the need. Presently there are many surface engineering techniques in use.

Classical surface engineering techniques:

- Casting
- Electro-plating
- Burnishing

Modern techniques

- Plasma coating
- Chemical vapor deposition(CVD)
- Physical vapor deposition (PVD)
- Sol-gel techniques

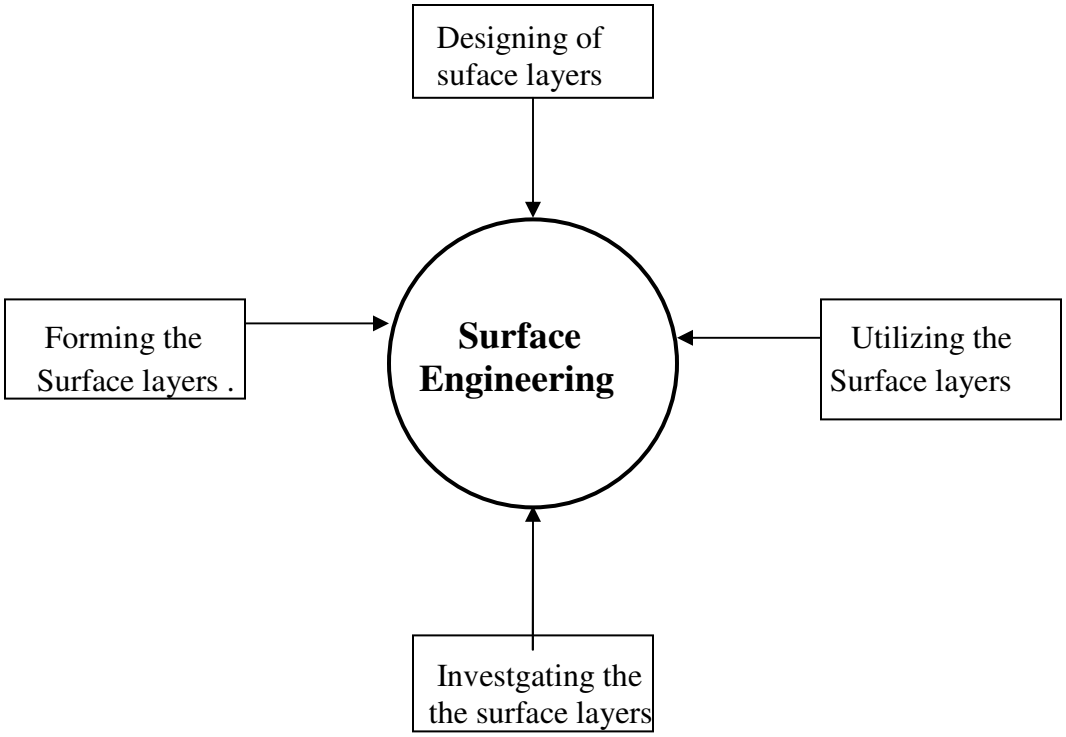

Figure 1.1: Schematic representation of the area of activity of surface engineering ref [1]

1.3 Coatings

Coating is a common method for creating better surface properties [1, 4, 7]. The concept of coating a surface is conceptually similar to the skin that covers the body of an animal to isolate it from its environment. Coating can be multi component or multi layer depending on the requirements. In some cases intermediate layers are used to improve adherence of the coating to the substrate [1].

1.3.1 Properties affected by coatings

Coating may affect many properties including [5]

- Mechanical properties: It can improve the wear-resistance, hardness of material.
- Optical Properties: Coating material can change the surface optical properties like refraction, absorption, and emissivity.
- Electrical Properties: Depending on the coating thickness it may affect the surface resistivity, conductivity and dielectric constant of the material.
- Chemical Properties: Protective coating can resist the corrosion and oxidation of a material.
- Material properties: The surface area and porosity of the material can be manipulated by coatings.

1.3.2 Requirements of the coatings materials

Many groups have proven that oxidation resistance of graphite can be improved by adopting various surface modification techniques of which the most promising is coating. Based on the research of Joshi and Lee, it was expected that ideal coating materials should have the following properties [21].

Mechanical Stability: At high temperatures the graphite structure becomes weak. This affects its mechanical strength so it is expected that the coating materials are mechanically stable.

Chemical Stability: Coatings should not under go any chemical reaction that can harm the substrate, and any coating should also be passive with the substance itself.

Adhesion: The adhesion between the coating material and substrate should be strong in order to provide thermal stability throughout operating temperatures.

Coefficient of thermal expansion (CTE): Cracks may form as a result of CTE mismatch between the coating and substrate. Hence the coating material is so chosen that it has CTE value close to that of substrate.

Permeability: Coatings are more effective if they have low permeability.

1.3.3 Classification of Coating

Coating can be classified in to various ways depending in the material or property targeted.

Based on material:

- Metallic, polymeric, composite etc.

Based on application [1]

- Protective coating involves shielding the substrate in corrosive, high temperature atmospheres and from wear.
- Decorative coating
- Protective & Decorative coating.
- Technical coatings can manipulate or improve like electrical, optical, and thermal properties of material.

Additionally classifcation can be based on the type of process used (fig: 1.2) e.g. CVD, electrolytic process, PVD, etc.

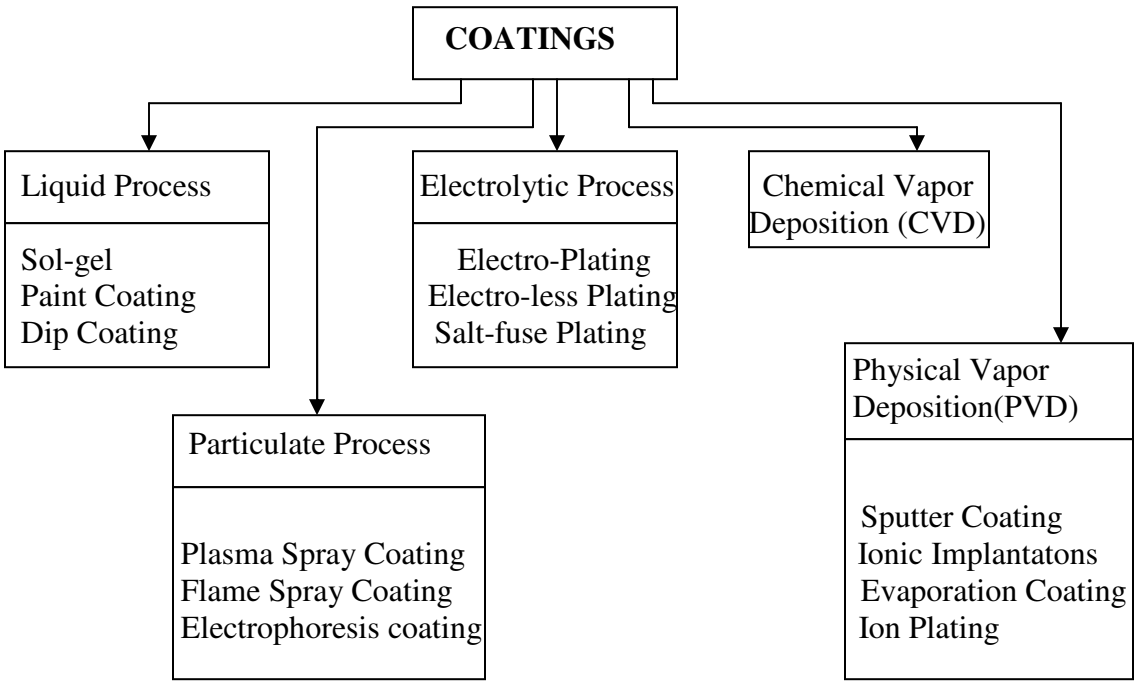

Figure 1.2: Classification of coating processes ref [5, 6]

1.4 Coatings on carbon foam

Surface modification is a general technique used to tailor the surface properties of various materials and is not new to traditional structures. For foam some studies have been reported. It was observed that the surface wettability and polar fluid infiltration of carbon foam was increased when the foam is etched with acids like HNO_3 because the acids bring oxygen functional groups to the foam [12]. By using plasma nano-coating, the carbon surface was manipulated to a great extent. Its surface turned active with Hexa-methyl di-siloxane (HMDSO) precursor and made passive with fluorocarbon coatings [15]. Carbon foam has variety of prospective applications in the field of electronics. It is prone to oxidation at high temperatures like other compounds of carbon (graphite, carbon fiber etc.). There are only a few groups that are working on the oxidation protective coating on carbon foam. The oxidation resistance of carbon foam was improved by James Klett et al. with SiC coatings using a methyl trichlorsoilane precursor [11]. There are several studies works in the area of oxidation protective coatings for carbon structures such as graphite and fibers. It is shown that graphitized foams are made up of stacked some graphitic planes [12]. In view of chemical similarity among these materials various possible coating on other carbon materials were compared before deciding a coating scheme for carbon foam.

1.5 Protective coatings on graphite parts and fibers

The oxidation of carbon compounds can be divided to three regimes [42]. The first one is low temperature oxidation (below 700^{o}C) that can be restricted by using boride like inhibitors. The second one is (between 700^{o}C and 1000^{o}C) where oxidation occurs by diffusion mechanism; this can be controlled by ceramic compounds. The third one occurs at high temperature regimes (>1000^{o}C), oxidation can usually be reduced by silicon based coatings [42].Various materials used for coatings and some novel concepts are discussed in the coming sections.

1.5.1 Silicon carbide coatings

Silicon carbide is widely used as a coating material for graphite because of its oxidation resistance, high thermal conductivity, and also its chemical compatibility with carbon. However cracks have been seen due to mismatch of CTE between SiC and C. Fergus et al. introduced a multilayer coating using a BCN inner layer surrounded by SiC which resisted the oxidation better than that of single layer SiC coating [27]. Most of the SiC coatings can have defects such as pores and pinholes. This was addressed by a three step process developed by Q Zhu et al (fig. 1.4) in which the substrate is primarily coated with SiC whose porosity is adjusted to fit the volume expansion when graphite converts to SiC [23]. It is covered with silicon slip to form a packed gel that can fill the pore. The entire setting was sintered to obtain a Si-SiC coating.

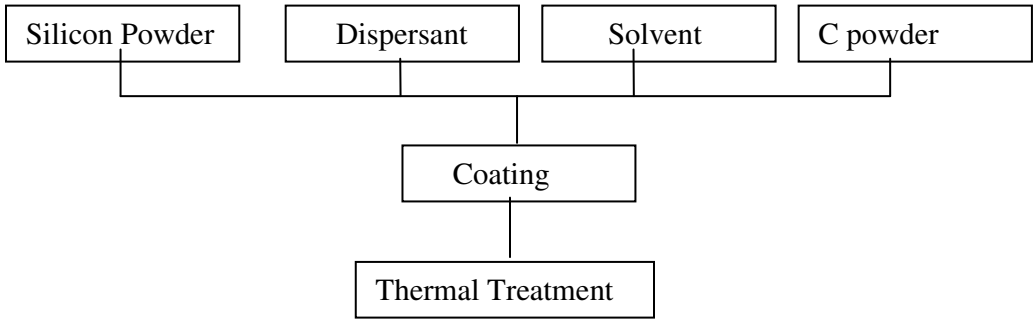

Figure 1.4: Three steps **SiC** coating developed by Zhu et al. [ref 23].

The formation of SiC by solution re-precipitation is a complicated mechanism. It was found that both the infiltration process and reaction rate determine SiC film continuity. The coating so obtained has good résistance to oxidation, thermal shock resistance and relatively inexpensive but can't withstand high temperature fracture.

SiC deposited at high temperature (above 1200^{o}C) can result in high tensile stress and lattice defects due to the mismatch of CTE between SiC and graphite. Boo et al tried to deposit the SiC coating at lower temperatures using a single source precursor hexamethyldisilane (HMDS) [24,25,26]. HMDS has a vapor pressure and so coating was done using both Metal Organic Chemical Vapor Deposition (MOCVD) and Plasma Enhanced Metal Organic Chemical Vapor Deposition (PEMOCVD). In PEMOCVD the substrates were pre-treated with argon plasma because it can increase the adhesion

between the SiC and substrate. The coating so formed improves the oxidation resistance of graphite. When the MOCVD and PEMOCVD processes were compared, it was found they have many advantages including:

- The coating obtained by PEMOCVD is crystalline while that of MOCVD is amorphous.
- Thicker films were obtained by PEMOCVD when compared to MOCVD.

Another coating technique, pulse chemical vapor deposition, has been also used for oxidation resistant coatings. It has an edge over the usual CVD processes because coatings have higher penetration capability into substrates and they are strongly bonded with the substrate. A pulse-CVD deposition of SiC formed from methyltrichlorosilane on carbon fibers has been reported [50]. The SiC layer formed here has good adherence with the carbon fiber due to anchor locking effect. Glass sealing of micro cracks formed during pulse-CVD made the coating effective at 1973^{o}C

1.5.2 Slurry coatings

It has been noted that one of the reasons for the failure of a coating is the difference in CTE between coating and substrate. These result in the formation of cracks which oxygen can penetrate to attack the structure [21]. Instead of ceramic coating, Joshi & Lee tried slurry-coatings on graphite that were already proven to be successful with refractory metals. They prepared the slurry by mixing Si, Cr, Hf, binder etc and applied it to graphite. It was found that the coating seemed to interact with the graphite, resulting in the formation of metal carbides at the interface. Though this appears to reduce the

oxidation of graphite to some extent, substrate fractures form and can develop into cracks. To overcome this, the concept of "discontinuous cracking" was introduced to control the degradation. In multiphase mixtures, cracks were arrested before they reached the substrate by introducing obstacles in order to achieve discontinuous cracks.

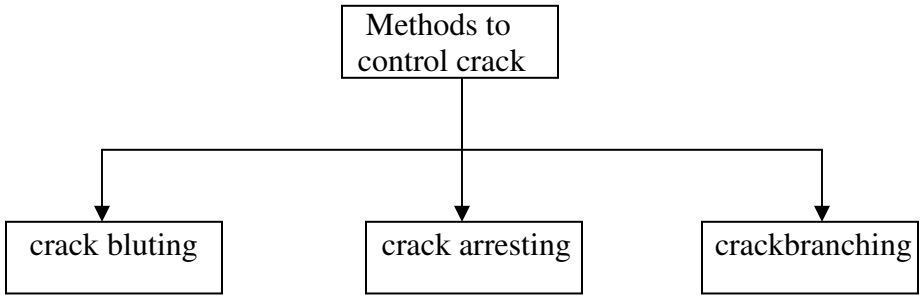

Figure 1.3: Methodologies to control fracture [21].

1.5.3 Phosphorous based coating

It was found that several forms of phosphorous are effective in retarding the oxidation including H_2PO_5, P, and its metal mixtures. The oxidation inhibiting capacity of phosphorous compounds may be due to [29]

- Diffusion barrier which acts as a protective layer in preventing oxidation.
- Active site poisoning.
- Scavenging the impurities into phosphate salts.

Chung et al. improved the oxidation resistance of carbon materials by acid phosphate impregnation, which is simpler than normal CVD processes [28]. Here polycrystalline graphite and carbon fiber samples used as substrates are pre-treated with ozone which resulted in the formation of oxygen containing surface functional groups. The substrates were then treated with the solution of phosphoric acid and aluminum hydroxide. This results in the formation of a white aluminum phosphate hard coating.

Aluminum phosphates prepared using solution-precipitation methods were treated with a powder form of graphite [29]. After the evaporation of excess water, the powder was analyzed using thermo gravimetric analysis. It was found that by such treatment there is an improvement in oxidation resistance. The interaction between the carbon and halogens like chlorine was also studied to check the ability of halogens to reduce the oxidation. The adsorption of gaseous chorine on solid carbon surface can be physical or chemical [33]. It was observed that oxidation of graphite was retarded in the atmosphere of chlorine compounds such as carbon tetrachloride [34]. Gonzalez et al. observed that chlorine inhibits the oxidation of graphite, carbon black, and sucrose, and there is also an increase in ignition temperature [30].

1.5.4 Miscellaneous ceramic coatings

Silica and Zirconia coatings are also used to protect carbon compounds from oxidation. Here coating on carbon composites was obtained by pyrolysing the pre-ceramic methylsilesquioxane using sol-gel technique. The resulting film could resist oxidation up to 1200^{o}C. The effectiveness of the coating depends on processing conditions and coating parameters such as hydrolysis time and withdraw speed.

Kobayashi et al. generated a SiO_2 and borosilicate coatings on carbon with self healing capabilities that are stable up to 900^{o}C even in wet atmospheres [48]. Parashar et al. enhanced the oxidation resistance of C/C composites using Zirconia- Silicion based coatings by sol-gel process [49]. Low-cost solution based coatings of SiC on carbon fibers were obtained from polycarbosilane. The coating improved not only the oxidation resistance and strength of the carbon fibers, but also their wettability which may ease the composite preparation.

H.T.Tsou showed that SiC deposited by Plasma-Assisted Chemical Vapor Deposition (PACVD) may not be able to protect the carbon composites [46]. The presence SiO_2 with active hydrogen may result in porous coating. An Si_3N_4 over-coating is effective in defending carbon composites from oxidation up to 1200^{o}C. H.T. Tsou also synthesized PACVD B_4C depositions able to protect carbon substrates up to 900^{o}C and hybrid coating of PAVCVD- B_4C and CVD- Si_3N_4 can protect up to 1300^{o}C [47].

Baklanova [39] synthesized protective nano-level coatings on carbon bundles using ceramic materials like alumina, zirconia, and silica using Sol-Gel techniques. The coating is homogeneous and has good adherence with the carbon fibers. But with sol-gel, multiple immersions may lead to overgrowth, which can develop mechanical stresses. Also such coating may obstruct the penetration of matrix material, which may lead to weak mechanical behavior of composites.

Konno etal grew Si-C-O composite films on the exfoliated graphite increasing resistance towards oxidation and allowing longer life in comparison to normal surface treatments [31]. Two types of silicone compounds with traces of Pt catalyst were impregnated into exfoliated graphite by absorption and then cured between $1000^{o}C$-$1400^{o}C$. The coating thickness was estimated to be few nanometers. The coating so formed has shown some anisotropic conductivity, which can be comparable to that of metal oxides. Oxidation tests performed on these samples showed decrease in weight loss due to oxidation.

1.5.5 Silicon oxide coating

Because of its interfacial stability with graphite at high temperatures, silicon oxide is also one of the choices for coating. Using atmospheric pressure CVD (APCVD) SiO_2 was deposited using Tetraethyl orthosilicate, which is less toxic when compared to silane or cholorsilane as precursor with a carrier gas [18]. Since APCVD is a high temperature thermo-chemical treatment there is a thick deposition rate due to high vapor pressure reactant gases. This technique works for both metals and non-metals. The coating so

obtained was observed free of cracks because of granular texture that deflects the stress energy. T.L. Dhami et al. studied the oxidation resistant coatings on carbon-carbon composites [51]. It was found that phosphorous oxide coatings derived from $POCl_3$ were effective up to 600^{o}C. SiC is a suitable coating material for use at higher temperatures that can be made more effective when the cracks were sealed. The boron based glass coatings serve this purpose by forming boron oxides.

1.5.6 Multilayer coatings

The concept of multilayer coatings was also applied on carbon materials to make them durable against the oxidation. In multi-layer and multi-component coatings each of the material is specially selected to optimize the performance. The first layer of coating is selected so that its linear thermal expansion is comparable to that of substrate there by minimizing thermal stress. It is expected that this first layer can adhere strongly to the substrate and also support the top layers. The second layer is supposed to have high thermal stability, heat resistance, and good interfacial properties (fig 1.5). The outer layer should have healing properties that can fill any crack formations during thermal loading [36, 37]. Other requirement of protective layer can be [38]:

- Diffusion barrier against fluids.
- Chemically compatible in terms of wettability, stability.
- Similar thermal expansion.
- Low permeability.
- Low intrinsic oxidation.

Multi layer coatings on a porous base coating below a dense coating can be a good approach. Here the porous base can serve as structural link between the carbon substrate and coating crest. Thermal energy plasma has generally been used to obtain a porous coating. The CVD process can used to obtain a dense layer coating on the top.

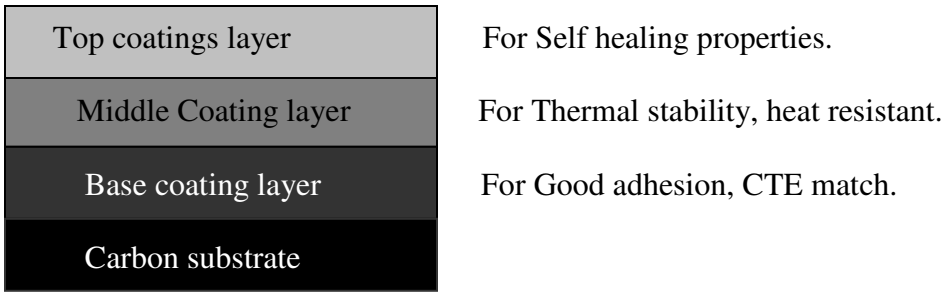

Figure 1.4: Schematic idea of multi-layer coatings [40, 41].

F.J. Buchanan et al. used a new approach in protecting the carbon composites by developing a multilayer coating using SiC and boron compounds [45]. The B_2O_3 that was usually used as a sealant has some problems including sensitivity to low viscosity and volatility at high temperature [35]. These difficulties were overcome by using glass compositions consisting of boric metals that can act as sealants over SiC.

Carbon fiber reinforced composites (CFC) have a wide range of applications, but like other forms of carbon they are prone to oxidation at high temperature. A multi-layer coating consisting of pyrolytic carbon, hafnium-carbon deposited by CVD, and SiC from methyl-tri-choloro silane and hydrogen was deposited on CFCs [36]. A mixture of SiC/HfC was observed at the interface which is a good sign for adhesion between the coatings. These multi-layers were able to pass thermal tests at 1450^{o}C in the atmosphere of SiO_2 with negligible mass losses.

For the protection of carbon composites, Guo et al. developed multilayer coatings using mixtures of borates and glass [35]. They addressed difficulties with ceramic coatings due to mismatches in thermal expansions that may develop cracks under cyclic loads. A self healing borate that has low viscosity and good wettability was used to fill the cracks. Protective multi layer coatings were developed using glass and borates. It was found that B_2O_3 formed on the surface resists the entry of oxygen.

It should be noted that porosity in coatings and substrates influences the oxidation of carbon composites. Both outer surfaces and inner surfaces of the composite are prone to oxidation due to porosity. A thorough study was made by Zmii et al. in this direction and they developed a complex coating from vapor impregnation through a liquid phase leading to increased strength and heat resistance in carbon composites even at elevated temperatures [37]. Using a eutectic mixture of Cu and Ni with B and Si in a liquid medium and at 1150^{o}C-1350^{o}C, liquid impregnation was accomplished.

1.5.7 Functionally gradient coatings

A novel multilayer coating consisting of graded SiC inner layer and a refractory oxide as the outer layer was developed by T.Morimoto et al. [40]. The graded SiC coating was obtained by converting a pre-deposited carbon layer into SiC by diffusion. The SiC coating so formed minimizes the CTE disparity between the SiC and carbon, thereby reducing the thermal stresses. A refractory outer layer of lanthanoid was used because it has high melting point, low evaporation rate and low oxygen diffusion rate. CTE mismatches of SiC and graphite are overcomes by this kind of graded coatings.

SiC concentration gradient coating concepts were also used by O.Yamamoto et al. in developing anti-oxidation coatings in carbon composites [41]. Here SiC gradient coating were obtaining by heating the carbon composites embedded in Silicon at 1450^{o}C in presence of argon similar to the T.Morimoto [40]. The substrates were then dip coated in zircon solution, which results in the formation of zircon films. The performance of composite coatings of SiC and zircon in terms of oxidation protection was a function of zircon coating thickness, and it is proven to be effective in protecting the substrates up to 1400^{o}C.

W.Kowbell used a novel method to obtain functionally gradient silicon based coatings using CVD and chemical vapor reaction (CVR). While both methods resist oxidation up to 1650^{o}C, on one hand, CVR uses non-toxic precursors and is a low cost one while CVD coatings are more dense and impermeable coating [42].

Zhu et al. were able to get functionally gradient SiC+Si_3N_4 layers using silicon infiltration technology [43]. In this, silica was made to react simultaneously with substrate and ammonia resulting in the formation of Si_3N_4 + SiC. The coating so obtained exhibited thermal shock resistance up to 1550^oC and good oxidation resistance on the C-C composites. A non crystalline C-Si functionally gradient coating was developed by S. Chu et al. using CVD technique [44]. This coating improved the oxidation resistance and tensile strength of carbon fibers. The interface soft layer between the C-Si coating and substrate was introduced to prevent the crack from being hitting the carbon fibers.

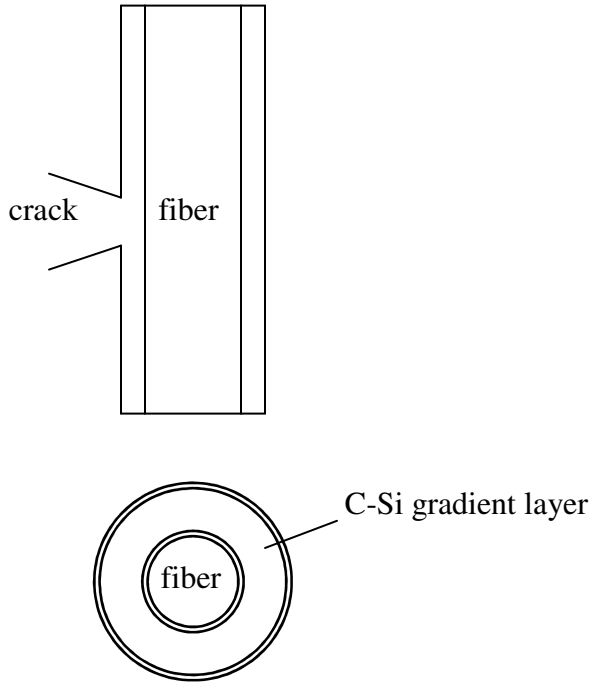

Figure 1.5: Idea of soft intermediate layer to prevent the crack hitting the carbon fiber surface [44].

Yamamoto et al. obtained SiC gradient coating on carbon materials which improved their oxidation resistance up to 1400^{o}C [41]. The oxidation resistance was pushed to 1600^{o}C by over coating the SiC-gradient coated substrates with mullite [49]. Mullite was impregnated into the substrates by soaking in a precursor solution prepared from aluminum nitrate and silicon tetra-ethoxide (TEOS).

It is observed that Silicon carbide is a widely used coating material in most of the processes. But there are some disadvantages with SiC coating: as they involve toxic precursors and need vacuum like pressures, during the coating process.

1.6 Boron Nitride as a coating material

1.6.1 BN Structure

Boron-Nitride is analogous to carbon in terms of its structure and electronic configuration. It exists in the form of hexagonal and cubical forms. With the hexagonal form is similar to graphite, and the cubical form similar to diamond. Hexagonal BN has an arrangement of boron and nitrogen two dimensionally in six member ring that are stacked in layers, so that nitrogen of one layer is over the boron of another layer in sp^2 hybridization. Cubic BN that is iso-structural to diamond has sp^3 hybridization. Like carbon, BN has some amorphous phases that can be converted to crystalline phase by annealing [52,53].

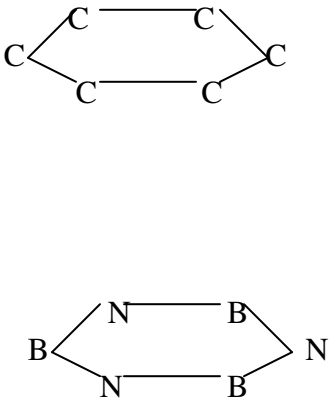

Figure 1.6: Similarity in structure between Hexagonal BN and graphite ref [52].

1.6.2 Applications

BN has a wide range of applications as [52,53].

- Lubricant
- Anti corrosive material
- Oxidation resistant coatings
- Dielectric material
- Lithograph masks
- Composites
- Sensors

1.6.3 BN coatings

The chemical inertness of BN at high temperatures has attracted researchers in developing anti-corrosive BN coatings. BN coating on steel and graphite substrates where synthesized at low pressures using r.f. plasma by Gafri et al. [54]. NH_3 and BCl_3 are used as precursors at 600^oC and the coatings formed are predominantly amorphous with little traces of crystalline h-BN. Gibbs free energy theory predicts thermo-dynamical succession of amorphous BN to hexagonal BN and then to cubic form. D.R. McKenzie et al. produced cubic BN films based on this Gibbs free energy theory [55]. B. Bonnetot et al. prepared BN coating from precursor mixture of tris-methyl amino borane and trimethylborozine which in turn were obtained from BCl_3 and methyl amine [56]. The precursors at a specific molar ratio have good wettability with graphite which may be ideal for impregnation. The boron nitride films so obtained were annealed at 1700^oC to

convert them from amorphous phase to crystalline phase. Substrates with such coatings have shown better corrosion resistance.

Using ion beam and vapor deposition (IVD) process BN thin films were produced on Si wafer substrates that are predominantly cubic. It has been shown that such BN multi layer films can improve the oxidation resistance [57]. Cubic boron nitride layers were developed using RF magnetron sputtering with Boron targets. In this process parameters like gas pressure, flow rates, composition and substrate temperatures may play a key role in controlling the coating growth [58]. BN films were also synthesized electro-dynamically using accelerated BN powder in a coaxial pulse plasma generator. The substrates are heated by the kinetic energy generated in the co-axial accelerator [59]. Multilayered BN coatings were deposited on SiC fibers by means of low pressure chemical vapor deposition from ammonia and boron tri-chloride mixture. The layers so deposited have lamellar structure consisting of successive stacks of isotropic and anisotropic BN layers [60].

Typically boron nitride films are synthesized from the constituents of boron and nitrogen from various sources. Usually precursors used for boron are boric acid, boric oxide, and boric halogens such boric chloride and boric bromide. Nitrogen can be derived from precursors such as ammonium and other organic compound e.g. urea or thiourea [72]. Boron nitride can be deposited on wide varieties of substrates including silicon which has extensive applications in electronics. Other deposition methods of BN on different substrates are to be discussed in this section. Boron nitride films can be synthesized on

silicon substrates with plasma assisted chemical vapor deposition [61]. The carrier gases used are BCl_3 and N_2 and the substrate is maintained at bias voltage. Here the coating process increased the surface roughness an effect which may depend on deposition time. Negative electron affinity was observed on BN films so deposited when processed with H_2 plasma and O_2 plasma treatments.

Berns et al. have grown cubic BN films on pure silicon substrates using low density supersonic plasma jet. Plasma can be generated at low temperatures with direct current arc. The arc is operated at the down stream of the expansion nozzle, based on gas mixture source consisting of argon and nitrogen with boron tri chloride. The deposition process is sensitive to substrate temperature and substrate bias voltage [62]. The films so obtained have nano-crystalline morphology, and compressive stresses which can lead to stress relief cracking.

Phase evolution of cubic boron nitride films on silicon wafers during r.f.-bias sputter deposition has been studied by examining the surfaces of BN films in three different growth stages [63]. In the initial stage a sp^2 bonded layer grows simultaneously, changing itself into argon blocking pre-cubic structure. In the intermediate stage, surface smoothing occurs when sp^3 bonded layer is formed from the sp2 bonded layer. Finally, a high stressed BN coating grows in to a single phase. J. Ye et al. prepared BN films on Si substrates without heat treating the substrate [64]. During the process, the Ar gas was used as working gas, and r.f sputtering was achieved using hexagonal BN targets. The cubic boron nitride can be obtained within a narrow gap of substrate bias voltage. Cubic

boron nitride of 90% yield can be obtained by carefully controlling the deposition parameters. It was observed that bias voltage gap increases with increase in Ar pressure. Osamu Tsuda et al. prepared cubic boron nitride films in a similar fashion on Si substrates, based on radio frequency (r.f.) bias sputtering [65]. In this process hexagonal boron nitride targets were used in pure Ar discharge in the presence of a magnetic field. The r.f voltage phase applied on target and substrate electrodes is regulated accordingly. The growth rate in this process is larger compared to the other PVD and CVD techniques reported.

Another processing technique for growing BN thin films is mass separated ion beam deposition (MSIBD). Such coatings can be applied on heated Si substrates in an ultra high vacuum environment [66]. This process seems to be better than other techniques for BN because it has some unique features:

- Isotropic pure ions of B and N are deposited.
- No other additional ions like Ar are required.
- B deposited as an energetic ion.

The film stoichiometry can be modified by controlling the B to N ion flux ratio and ion energy control.

The effect of substrate in the deposition of BN was studied by P. B. Mirkarimi et al. [67]. They deposited BN films on wide range of substrates by ion assisted plasma laser

deposition technique. It was found that BN film growth on metals is lower compared to growth on Si or SiC substrates. BN growth here depends on micro hardness of the substrates.

Thin films of boron nitride were grown by S.B. Hyder and T.O.Y ep using reactive plasma deposition which follows the ammonia diborane reaction [68]. The substrates used were silicon, compression-annealed pyrolytic graphite, and compression-annealed pyrolytic BN. The largest crystalline BN grains appeared on pyrolytic BN grains.

The reaction occurred may be:

$$B_2H_6+2NH_3 \longrightarrow (NH3)_2H_2 + BH_4 \text{ (low temperature)}$$

$$B_2H_6+2NH_3 \longrightarrow 2BN+H_2 \text{ (high temperature)}$$

MF Plass et al. synthesized thin boron nitride films using ion beam assisted deposition. They studied the layered growth in BN films i.e. cubic BN on top of non cubic BN whose ratios are determined using some analytical methods [69]. B. Choi deposited hexagonal boron nitride on graphite substrate by reacting ammonia with boron nitride in reduced pressure at temperatures 800^{o}C to 1200°C [70]. The growth rate of h-BN films is dependent on the substrate temperature and pressure. It was said that the growth rate increases with increase in substrate temperature. The temperature at which the maximum growth rate occurs decreased with increasing total pressure. With increase in substrate temperature and total pressure, the grain size and surface roughness are increased.

High temperature behavior of hexagonal boron nitride was studied by Milan Hubacek et al. [72]. It was reported that crystallization of BN proceeds in steps that consist of formation of semi-oligomers of boron and nitrogen, which further coalescence and whose mechanism can determine crystallinity of BN films. The structure of BN is determined by interaction between the BN mono-layers and their chemical interaction with the environment. BN films on the silicon substrates can be deposited by metal organic chemical vapor deposition (MOCVD) according to K Nakamura et al. [73]. Precursors used are mono methyl hydrazine (MMH) and triethylboron (TEB) that are the sources of nitrogen and boron respectively. However, the crystals so formed were inferior to the films formed when ammonia was used as nitrogen source instead MMH.

F. Rossi et al. used the plasma assisted chemical vapor deposition (PACVD) to build films of boron nitride on the single crystal wafers of silicon from BCl_3 and N_2 which are precursors of $N_2$and H_2 [74]. They achieved some success in synthesizing low residual stress films at low bombardment energies. Ion flux and ion energies were measured by estimating the transition states of h-BN and C-BN. For the first time thin cubic BN films with out SP^2 hybridization were obtained by I.Konyashin with plasma assisted chemical vapor deposition on Silicon substrates [75]. The precursors used here is dimethyl borane or borane ammonia in hydrogen plasma. The structure of films so obtained depends on the ratio of precursor to hydrogen.

A Low pressure chemical vapor deposition method was adopted in building BN films on graphite by J.L. Huang et al. [76]. Amorphous films were obtained when treated at 1100^{o}K. Those films so obtained are transformed into hexagonal phase when heat treated at about 2023^{o}K. The transformation depends on the duration of heat treatment. The kinetics of concentrations of BCl_3, NH_3 are determined in order to optimize the growth rates. The effects with and with out carrier gases H_2 and N_2 were also studied.

Nechepurenko et al coated the graphite samples by using graphite as the reducing agent for born oxide vapors in the atmosphere of nitrogen [77]. They obtained the BN coating by sintering and heat treating graphite substrates in presence of boron oxide and ammonia gases. Here BN coating improved the oxidation resistance of graphite up to 10 times. Nechepurenko et al. tried to inhibit oxidation in graphite by coating it with boron nitride [16]. BN is a good choice because it is not wetted by most of the non-ferrous metals. Coatings obtained by heat treating the specimen in a sinter made with an N-R compound and B_2O_3. The N-R compound here acts as a nitrogen source and it allows lower operating temperatures. They improved the oxidation resistance by a factor of about 12 at 1200^{o}C.

1.9 Objective of the Thesis

At high temperatures carbon structures like carbon/graphitic –foam and graphite are prone to oxidation due to oxygen present in air which may weaken their strength and other mechanical properties. Coating is one such remedy that can reduce the degradation of a material. Little attention has been given porous structure like carbon foam which is sensitive to oxidation. Various combinations of HMDSO coating ranging from 20nm to 240nm were tried. It was found an HMDSO coating does not help in reducing the oxidation of the carbon foam. An alternative process based on liquid phase process BN coating using PVP binder is developed. This coating is simple, easy to process and non-vacuum based. A multi layer coating using different sizes of BN particles was studied. The coatings are analyzed based on the surface morphology and performance. The coating is applied on both carbon and graphite foams.

2 EXPERIMENTAL PROCEDURES

2.1 Overview

This chapter gives a detailed account of the procedures followed while setting up the experiments. It also gives in-depth description of characterization techniques and analytical methods in accomplishing the results.

2.2 Preparation of substrates

Samples of a standard sizes 0.5 cm cubes are prepared from carbon foam chunks. Graphite samples are also used for checking the surface morphology and coating chemistry. The graphite samples were cleaned before applying coating by ultra-sonication, in acetone for 10 minutes and then in methanol for 10 minutes.

2.3 Plasma coatings

Plasma coatings were carried out using a plasma microwave chamber from Plasma Tech Inc. The micro wave consists of a rectangular microwave chamber below which is a vacuum chamber and there are glass flow lets in to the vacuum chamber (fig 2.3(a)). The process consists of threes steps: surface activation deposition and stabilization of coating. This process is explained below:

- Process 1: This step is intended to clean and activate the sample surface by gas which gets ionized inside the microwave chamber. For this process oxygen was used at a pressure 50Pa, flowing at 48ml/min and micro power used is 225 W.

- Process 2: The oxygen along with the HMSO is passed in to the chamber at flow rates of 50ml/min and 2ml/min respectively. The micro wave power is 250W and chamber pressure maintained at 50Pa. The process time here determines the thickness of coating.

- Process3: The coating was stabilized by passing O_2 gas for 1 minute at 150w at a flow rate of 48ml/min.

The following table gives a detail account of values of parameters used.

	Process 1	Process 2	Process 3
Base pressure	15 Pa	15 Pa	15 Pa
Gas stabilizing time	20 s	20 s	20 s
Gas1(HMDSO)	0 ml/min	2ml/min	0ml/min
Gas 2(oxygen)	48ml/min	48ml/min	48ml/min
Process pressure	50 Pa	50 Pa	55Pa
MW power	225W	250W	150W
Process time	180s	Variable	60s

Table 2.1: Parameters used for plasma HMDSO coatings.

Figure 2.1: Plasma Tech coating microwave used for HMDSO plasma coating.

2.4 Solution used for BN coatings

Several solvents were tried in the beginning in order to identify the most promising method. Methanol was the first one since it is one of the simplest solvents that evaporated without residue. The methanol-BN is prepared by dissolving 0.3g of 1µ size BN particles in 10 ml of methanol. The solution is then stirred for about 10 minutes using a magnetic stirrer. The samples are then dip coated in the solution. For this purpose 1µ size BN particles are used (Aldrich Sigma Inc.). Other solvents that were attempted are Di-Ethyl Amine (DEA) and Xylene. It was seen that most of them, without any binder resulted in porous coating. Therefore a new process using an organic binder was investigated.

2.5 Coatings with solvent and binder (PVP in methanol)

0.15g of PVP powder is dissolved in 10ml of methanol to Poly-Vinyl Pyrrolidone (PVP of MP Biomedicals LLC.) solution. In PVP solution 0.3g of BN powder is added to prepare PVP-BN dipsersion. The sample is dip coated in the using the PVP-BN dispersion. The coated sample is placed in furnace and temperature is raised to 200^{o}C at rate of 5^{o}C/minute. The heat treatment profile is as shown in the fig-2.5(a).Then the sample is heat treated at 200C for 1 hour to remove the organics from the coating, and it is then air cooled to room temperature (fig 2.5(b)). The BN powders used are of size 1µ (Aldrich Sigma Inc.) and 0.7µ (Atlantic Equipment Engineers).

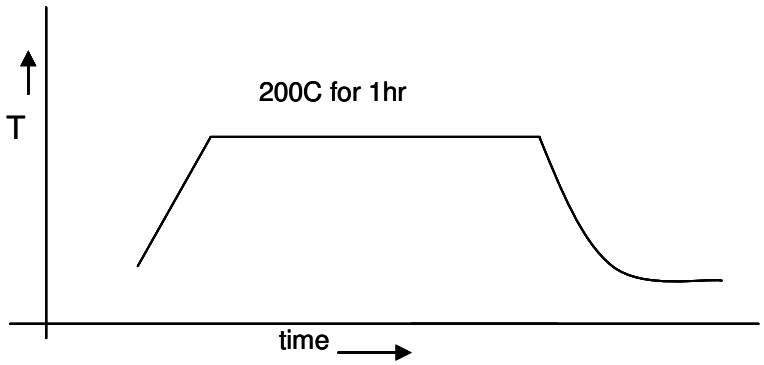

Figure 2.2: Heat treatment profile of PVP-BN coating.

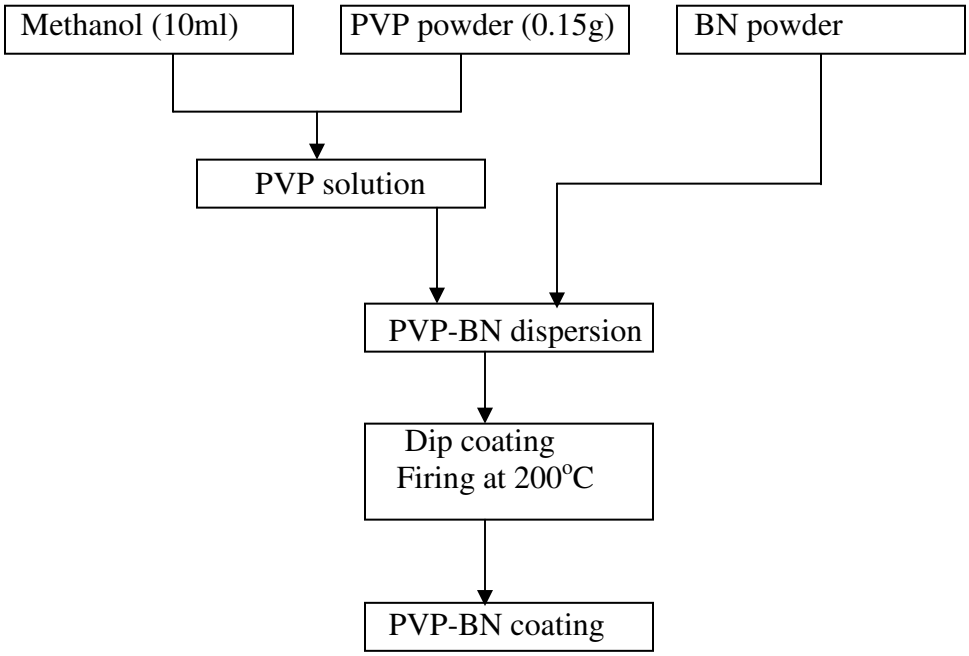

Figure 2.3: Process for preparing PVP-BN coating.

2.6 Characterization techniques

The characterization techniques used in this study are Scanning Electron Microscopy (SEM), X-ray Photoelectron Spectroscopy (XPS), and Field Emission Scanning Electron Microscopy (FESEM).

2.6.1 Secondary Electron Microscopy (SEM)

SEM is one of technique that is widely used for studying the surface micro-structure. In most aspects it is similar to an optical microscope. In SEM, an electron probe is used for rastering the surface of the specimen, which may lead to several kinds of emissions. The emissions (like back scattering electrons, secondary electrons) are mapped on the cathode ray tube correspondingly that results in the formation of an image.

Some of the details of Jeol SEM used here are [79]:

1. Illuminating beam: Electron beam.
2. Wave length: less than 0.006nm.
3. Medium: vacuum.
4. Lens: Electronic lens.
5. Resolution: For secondary electron image: 5nm.
6. Depth of field: 30µm.
7. Magnification: 10X to 180,000X.
8. Focusing: Electrical.
9. Obtainable images: Secondary electron and backscattered, electron images.
10. Contrast: Geometrical shape, physical and chemical properties.
11. Monitor: Cathode Ray Tube (CRT).

Figure 2.3: Process for preparing PVP-BN coating.

Figure 2.4: JSM-35CF Scanning Electron Microscope from JOEL Inc., USA.

2.6.2 X-ray Photoelectron Spectroscopy (XPS)

XPS also known as electron spectroscopy for chemical analysis (ESCA) is a surface analysis characterization technique based on photoelectron principle (fig 2.6.2). When the sample is irradiated with mono-energetic X-rays, electrons whose energy correspond to specific energy state an element are emitted. Physically in this process a known energy photon when interacts with the surface of a sample, some electrons of the sample surface are knocked out [80]. The kinetic energy of such emitted electrons is related to the binding energy of the electron a particular state as

$$E_{be} = h_v - E_{ke}$$

where, E_{ke} - kinetic energy of the electron

E_{be} - binding energy

h_v - photon energy.

The kinetic energy of photo electrons emitted is calculated based on electro-magnetic concepts. The binding energy which is a characteristic property of a particular state of an electron, found based on kinetic energy of emitted electrons. The binding energy so calculated can pin point the elements present on the surface of the sample.

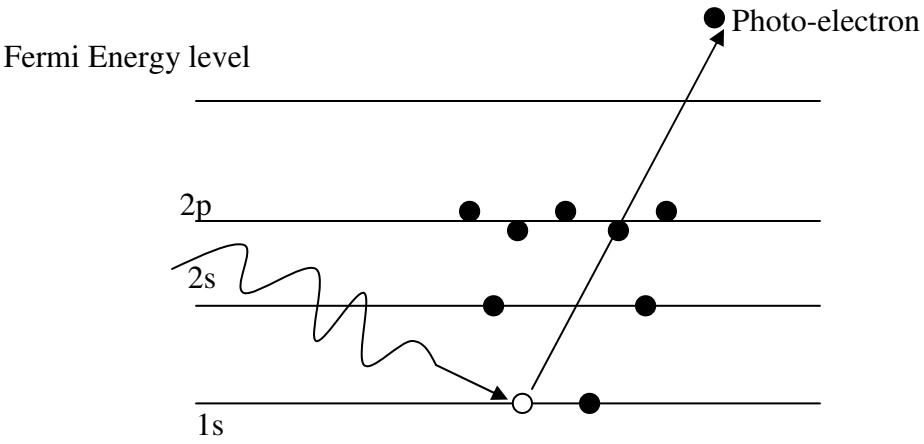

Figure 2.5: Photo-electron technique of XPS.

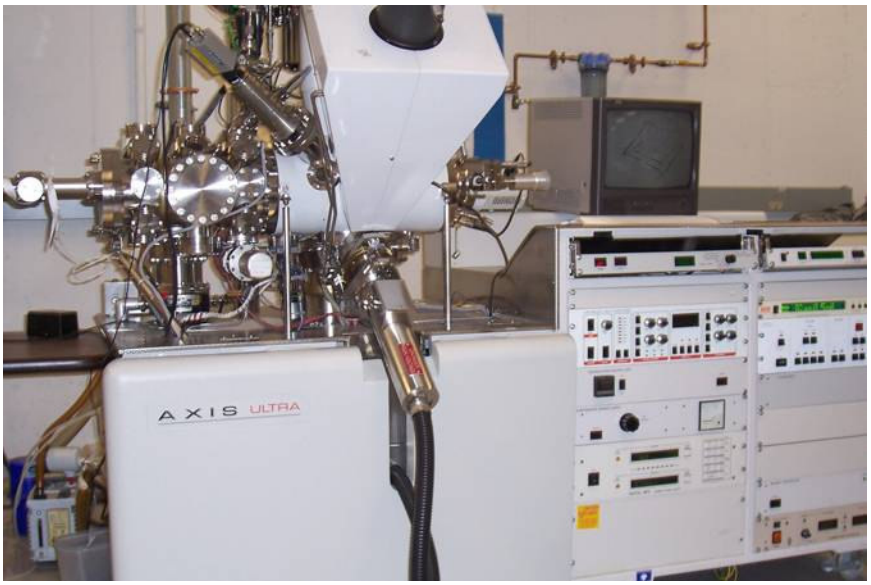

Figure 2.6: XPS ULTRA of KRATOS ANALYTICAL Inc.

2.6.3 Field Emission Scanning Electron Microscope (FESEM)

FESEM is also one of the characterization technique used in this study to observe the surface morphology of the coating. This JSM-7401F FESEM used here is a high ultra resolution SEM that employs a field emission gun as the electron source. This system integrates systematically the secondary electron detector, back scattered electron detector and secondary electron enhancer in order to acquire high definition information of the specimen. This system is operated on a graphical user interface (GUI) using a Windows based PC host.

3 RESULTS AND DISCUSSION

3.1 PLASMA COATINGS

3.1.1 Introduction

Studies have been conducted about the ability of SiO_2 coating in protecting graphite from oxidation using CVD process [18]. The TRL carbon foam samples that were plasma coated using HMDSO (hexa-methyl di-siloxane) under different coating times to deposit silicon oxide coatings. The samples are heat tested at 700^{o}C for 1 hour and also at 600^{o}C for 2 hours to check their effectiveness.

3.1.2 HMDSO plasma coating

Earlier investigation shows the relation between the coating thicknesses and coating times of the plasma coating [14]. They devised a set of experiments and analyzed the samples coated at different time intervals using XPS. After quantitative calculations it was found that the thickness of the oxide plasma coating can be approximated to 4nm for 1 minute of coating. Assuming the coating rate, 4nm/min (5, 10, 30 and 60 minutes) different coating times were used (tables: 1 and 2). The percentage of weight loss of the carbon foam heat treated in the furnace at 700^{o} for 1 hour is calculated and tabulated as follows.

Sample No.	coating time	assuming thickness(4nm/min)	percentage of weightloss (error ± 5)
1	Uncoated	0	48%
2	5 minutes	20 nm	53%
3	10 minutes	40 nm	54%
4	30 minutes	120nm	53%
5	60 minutes	240nm	51%

Table 3.1: carbon foam oxidation for different coating times at 700^{o}C for 1 hour.

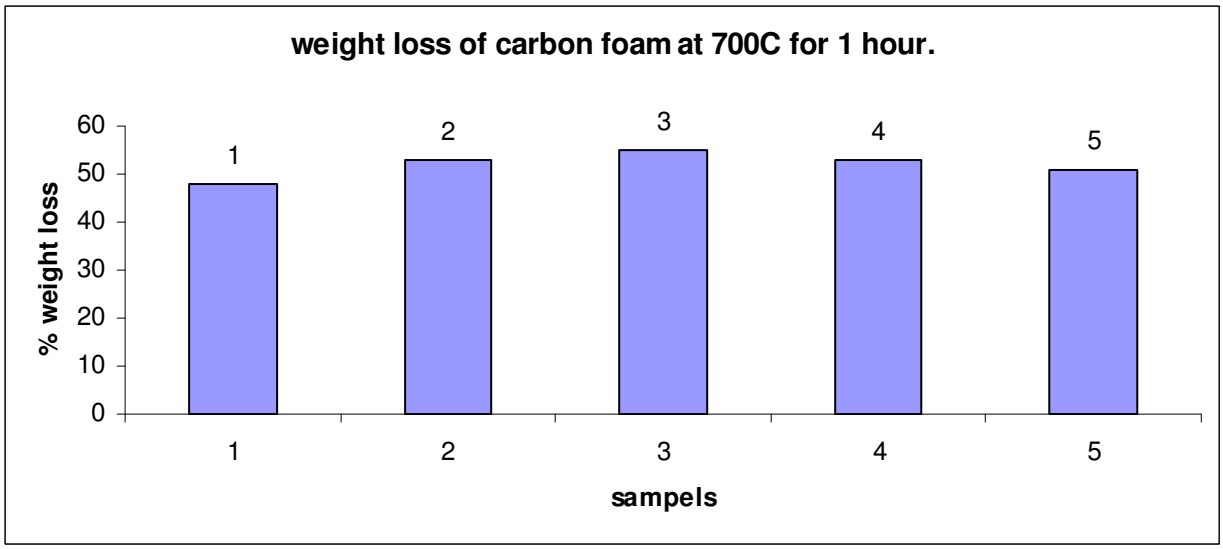

Figure 3.1: comparison of percentage of oxidation of TRL foam at 700C for 1 hour heat treatment.

.

The sample carbon foam which were coated for 30 minutes and 60 minutes were heat treated at 600°C and the percentage weight loss is calculated and tabulated as follow:

Sample #	coating time (minutes)	approximate Thickness(4nm/min)	percentage of eight loss (error ± 5%)
sample1	Untreated	0	13%
sample 2	30	120nm	18%
Sample3	60	240nm	23%

Table 3.2: Carbon foam oxidation for different coating times at 600°C for 1 hour.

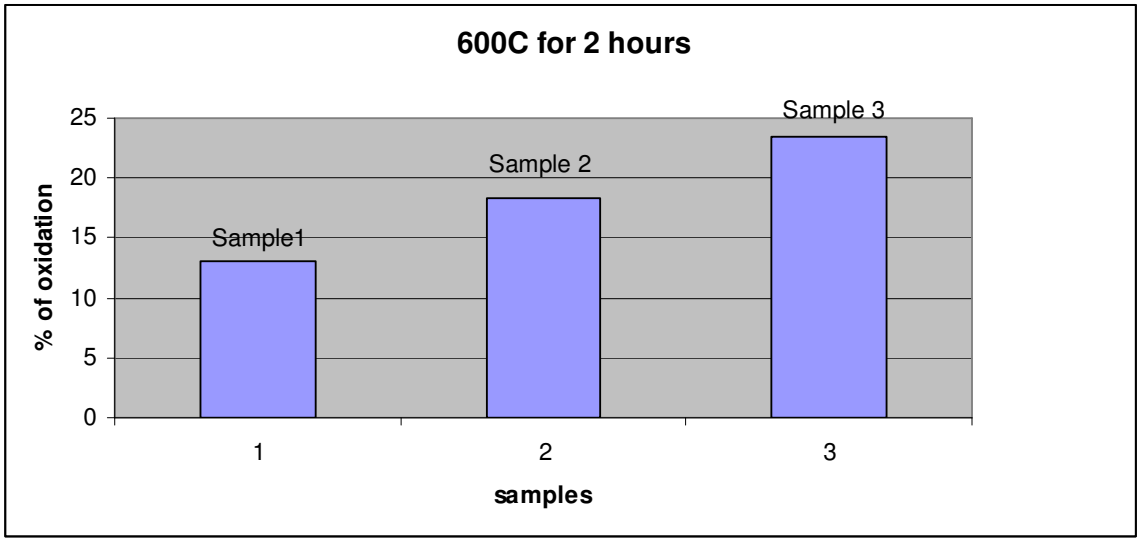

Figure 3.2: Comparison of oxidation percentages of TRL foam for different coating times at 600°C for 2 hours.

It can be seen that oxidation of the foam was increased to 53% and 54% for 5 and 10 minutes coating respectively. It was thought that the coating thickness was not sufficient to protect the carbon foam and hence coating time was increased to 30 and 60 to bring the coating thickness from nano-levels to micro levels. It can be seen that the weight loss is 53% and 51 % for 30 and 60 minutes coating times which is still higher when compared to that of uncoated foam (Figure:3.1, Table 3.1).

The HMDSO coatings are also tested at 600^{o}C for 2 hours. The uncoated foam show a weight loss of 13% while that of 30 minutes coated one shows a weight loss of 18% and 1 hour coated one shows 23% of weight loss. It may be observed the weight loss increased with coating thickness even at 600^{o}C (figure:3.2, table 3.2). The data clearly shows that HMDSO coatings are not for protecting the carbon foam oxidation but rather it aides in the process. In previous studies by R Pulikollu [14] it was shown that being an active one, SiO_2 plasma coating increases the water absorbability and carbon nanotube growth on the foam. Unlike normal SiO_2 coating, the coating obtained here at room temperature, is expected to be amorphous that may not inhibit oxidation. This is possibly the reason for the failure of nano scale (plasma deposited) silica layers conflicting to crystalline SiO_2 coatings in earlier studies [18].

3.2 METHANO BORON-NITRIDE COATING

3.2.1 Introduction

Many coating materials are in use to protect the carbon structures from oxidation of including SiC which is a widely used coating material for inhibiting oxidation on graphite. However SiC coating requires high temperatures and low atmospheric pressure during formation. Therefore, SiC coating is not considered here as a coating material. Other coating materials like Al_2O_3 and SiO_2 have similar difference in CTE with carbon as that of BN (Table 3.3). BN is one of the choices because of its inertness and chemical stability. Different type of Boron Nitride coating procedures was discussed in the previous chapter [chapter (1.6)]. It may be recalled that most of the processes use boron halides and ammonia as precursors. But precursors such as BCl_3, BBr_3 are not only expensive and corrosive but also toxic. So a new process that doesn't make use of toxic precursors was designed using the concept of liquid phase coatings. Dip coating was selected to obtain BN coatings as it is simple to process and control, permeable through foam and the least hazardous of given options.

	CTE at 20^{o}C ($10^{-6}/^{o}$C)
C	3
SiC	4
SiO_2	0.3
BN	8
Al	25-21
Ni	17-12
Al2O3	0.38

Table 3.3: Coefficient of thermal expansion of different materials at room temperature.

BN powder is mixed in a simple solvent. Methanol is used because it dries out easily due to its low vapor pressure at room temperature. Initially simple BN coatings are made using methanol and BN powder but no binder. Subsequently it was seen that methanol alone is inadequate and a binder was added.

3.2.2 BN coatings with methanol

The TRL-foam is coated using methanol and BN powder is heat treated at 700C for 1 hour. The weight loss of coated foam is found to be 53% while that of uncoated is 48%. The BN coated has more weight loss when compared to that of uncoated and thus proved that it is ineffective in resisting the oxidation at a high temperature like 700^{o}C. This time the coated is tested at low temperature i.e. at 600^{o}C for 2 hours. The BN coated foam loses 12% of weight loss while the bare foam loses 13% of weight. Unlike in the previous test, the weight loss in both the case is same is almost same (Figure: 3.3, Figure: 3.4). It appeared that adhesion between the foam and coating was poor and this could be one of the reasons for the ineffectiveness of BN coating here.

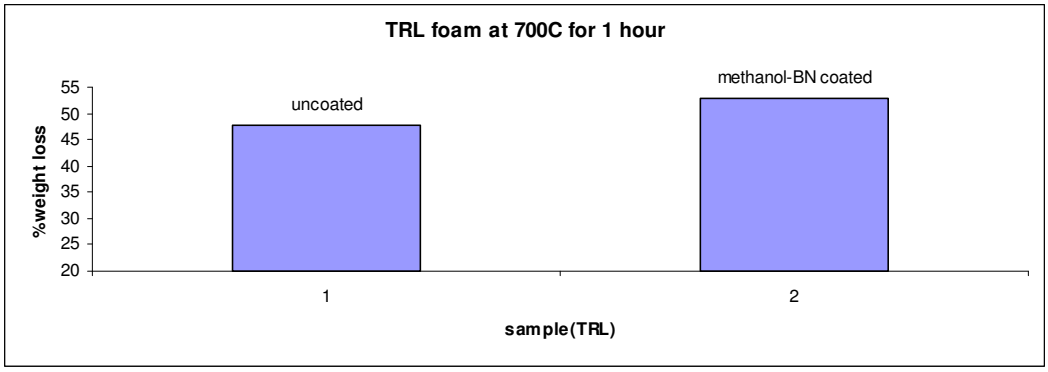

Figure 3.3: Comparison of weight loss of uncoated and methanol-BN coated TRL foam at 700^{o}C for 1 hour.

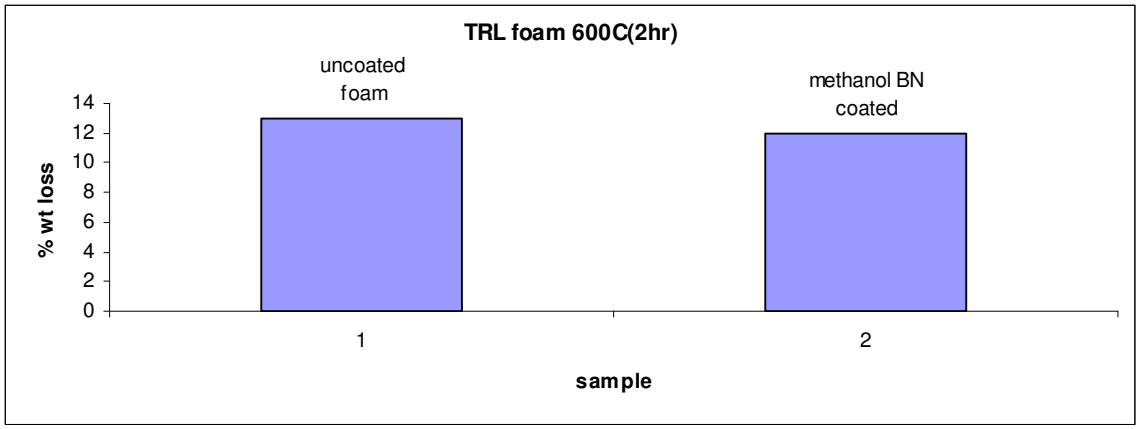

Figure 3.4: Comparison of uncoated and methanol-BN coating BN TRL foam at 600^{o}C for 2 hours.

To improve the spread-ability of the BN film, adhesion with the substrate a suitable binding agent is needed and that was what we looked.

3.3 PVP-BN COATINGS

3.3.1 Overview

It was seen in the previous chapter that methanol based coating without a binding agent does not enhance the oxidation resistance in the carbon foam. One of the problems with methanol coating was the poor adhesion obtained between the coating and the substrate. A suitable binder is needed to increase the adhesion between that of film and substrate. Here Poly Vinyl pyrrolidone (PVP) is selected as binder (Figure 3.5). PVP can act both as a binder and as well as a dispersing agent. When BN is mixed with PVP like cyclic compound, the PVP may interact with the BN particles resulting in formation of chain like compound that may break during subsequently during firing. This may result in the formation of BN films on the substrates. In this chapter results from studies of liquid based BN coating prepared based on polyvinyl- pyrrolidone (PVP) binder and BN powders are discussed.

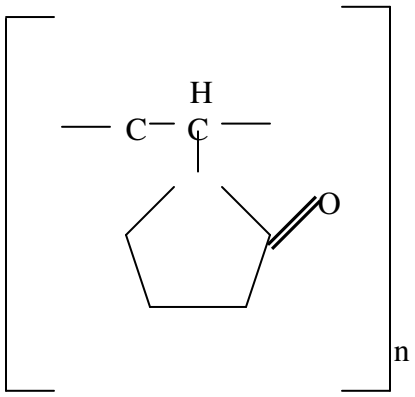

Figure 3.5: PVP structure

3.3.2 PVP-BN coating using 1µ BN particle

The Touchstone Research Laboratory (TRL) foam substrate is coated with 1µ BN particle using PVP-BN dispersion and then fired at 200°C for 1 hour. This process is repeated one more time, resulting in the formation of a double layer of BN coating as shown in figure below (Figure 3.6).

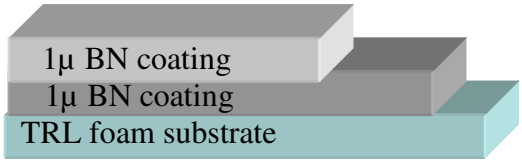

Figure 3.6: Coating scheme of PVP-BN coating on TRL foam

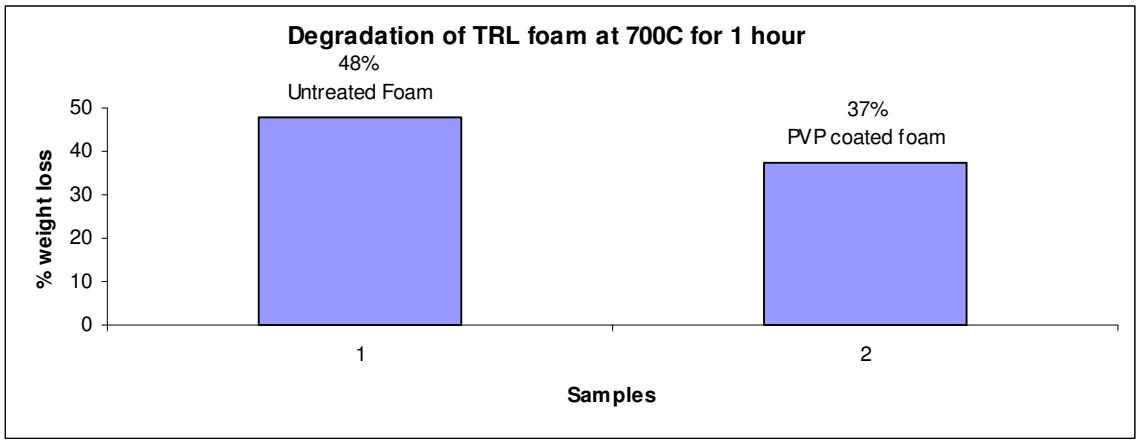

Figure 3.7: comparison of weight loss of uncoated and coated foam at 700°C for 1 hour.

The coating so formed is tested by heat treating at 700°C for 1 hour. The weight loss of as-received TRL foam is 48% .While under similar conditions the weight loss for coated foam is 37%. Weight loss decreases to 23% due to PVP-BN coatings (Figure 3.7). This

shows that PVP-BN coating works on the TRL foam in improving the oxidation resistance to some extent. Figure: 3.8 shows surface morphology of PVP-BN coating at 2000X taken using FESEM. The surface of the coating seems to have clusters that are much bigger than 1µ BN particles used for coating. Agglomeration of the particles is therefore suspected. A smaller particle size may help by providing more compact and refined layers.

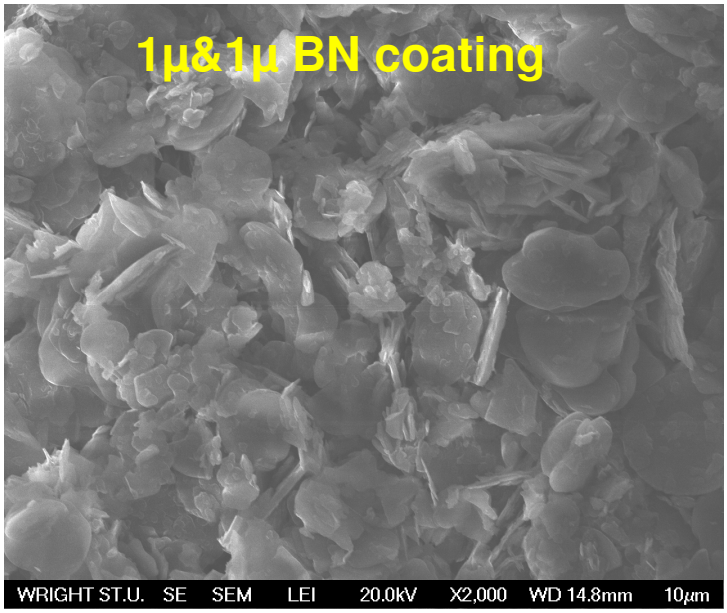

Figure 3.8: Surface morphology of two-step PVP-BN coating formed using 1µ BN powder at 2000X.

3.3.4 PVP-BN coating using 0.7 µ BN particles

The weight loss is decreased due to the PVP-BN coatings from 1µ BN particles. The coating is tried to using still higher purity and finer size particles may help.

The TRL foam sample coated using a dispersion of 0.7µ size BN particles and PVP solution was fired at 200^{o}C for 1 hour. This process is repeated one more time to get a double layer coating of 0.7µ size BN particles (Figure 3.9). The sample is heat treated at 700^{o}C for 1 hour and it weight loss is noted. The weight loss of PVP-coated foam is 32% while that of uncoated foam is 48% (Figure: 3.10). The decrease in weight loss is 33% due to the PVP-BN coating. In Figure:3.11 is shown the surface morphology of this coating, and it demonstrates that particle size here is comparatively smaller than the previous PVP-BN coating formed using 1µ BN particles. The weight loss here is also smaller than that of the PVP-BN coating formed using 1µ BN particles. The use of smaller particles may have reduced porosity thus resulting in improved performance.

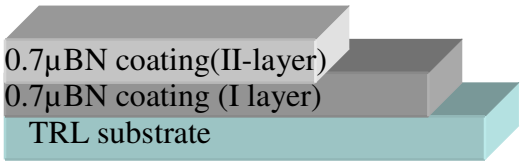

Figure 3.9: Coating scheme employed for PVP-BN coating using 0.7µ BN particles.

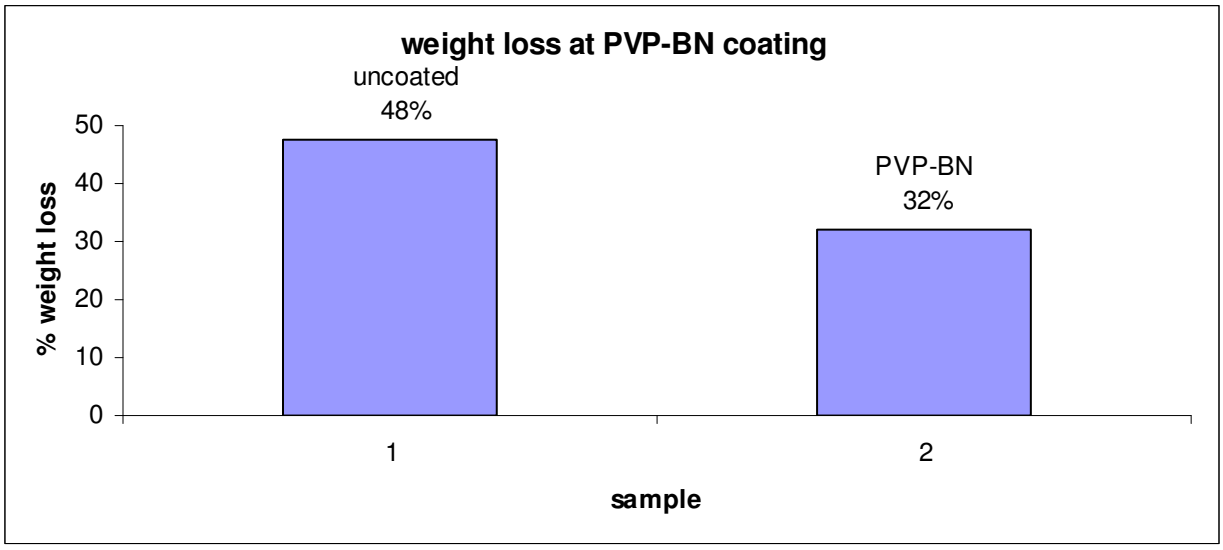

Figure 3.10: Comparison of weight loss of uncoated and PVP-BN coating using 0.7µ BN particles.

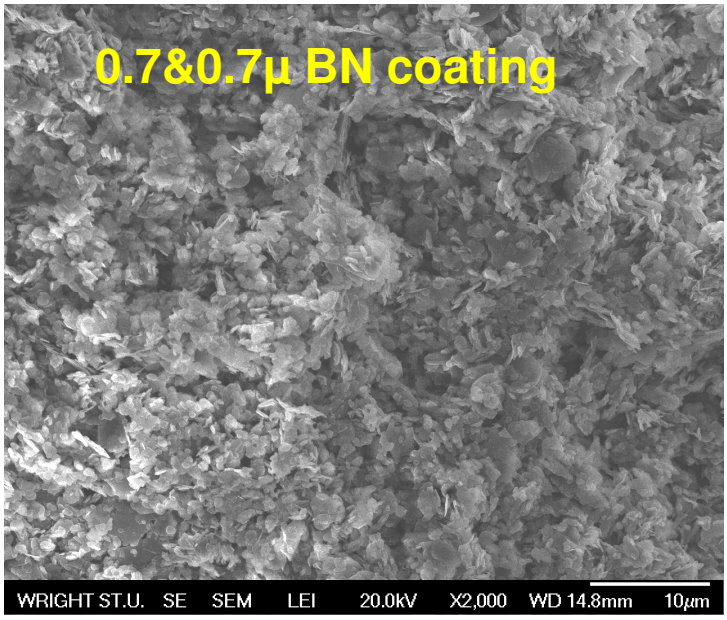

Figure 3.11: Surface morphology of PVP-BN coating using 0.7µ and 0.7µ BN particles at 2000X.

However there are still issues with porosity. It was therefore decided that a reasonable next step may be two layer coating where the first layer is formed using larger size particles (1μ) and second layer is formed using smaller size particles (0.7μ). Use of smaller size particles may fill the gaps.

3.3.5 PVP-BN coating using 1μ and 0.7 μ BN particles

The TRL foam substrate initially coated using 1μ size BN powder and PVP solution is fired at 200^{o}C for 1 hour. This process is repeated for 0.7μ that results in a coating scheme as shown in figure 3.9. The sample is heat treated at 700^{o}C for 1 hour. The percentage of weight loss of the coated one is 29% while that of bare TRL foam is 48 % (figure 3.14). The decrease in weight loss due to the coating is 40%. This combination works better than that of previous combinations. Figure 3.15 shows the surface morphology of this coating and this coating is finer than that of PVP-BN coating formed by just 1μ BN particles. Also surface morphology of this coating looks similar to that of PVP-BN coating formed using 0.7μ BN particles. Performance wise, this coating is better than the earlier two coating which may be due to reinforcement of 0.7μ BN particles over 1μ BN particle (Figure 3.13).

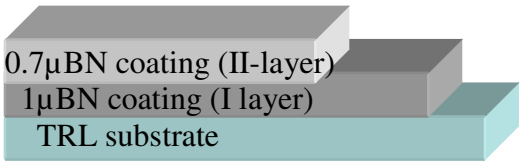

Figure 3.12: Different PVP-BN coating combinations using 0.7μ and 1μ BN particles.

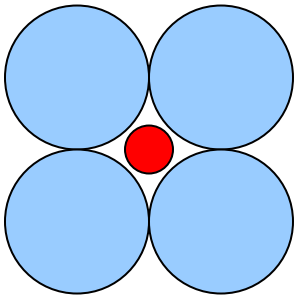

Figure 3.13: The bigger particles of 1are surrounded by smaller particles.

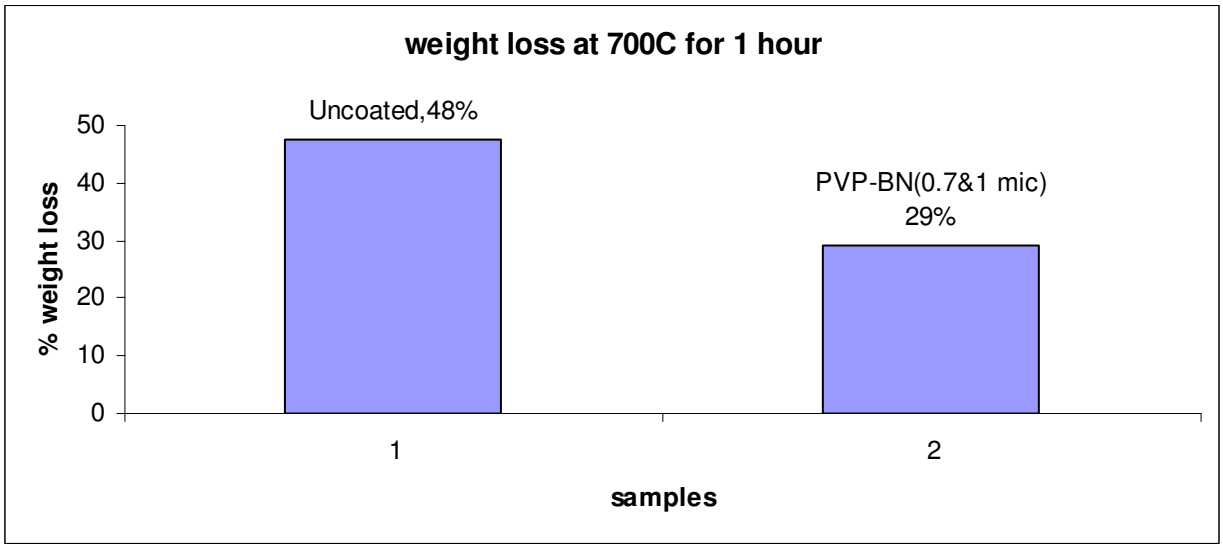

Figure 3.14: Comparison of weight loss of uncoated and PVP-BN coated TRL foam at 700^{o}C for 1hour

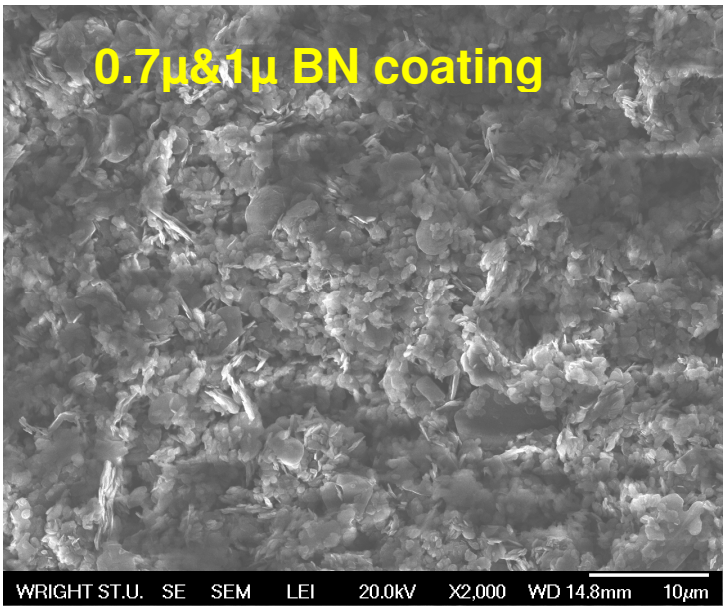

Figure 3.15: Surface morphology of PVP-BN coating using 0.7µ and 1µ BN powder at 2000X.

3.3.5 Surface Chemistry of the PVP-BN coating

3.3.5.1 Samples heat treated

The sample of PVP-BN coating of 0.7 μ and 1μ was analyzed using XPS to identify the elements present and their bonding states. Figure: 3.16 is the surface survey scan of double layer coatings of PVP-BN formed using 0.7μ and 1μ particle. In fig 3.3(j) shown are the elements present in the coating: Nitrogen, Boron, Carbon and Oxygen. The B 1s peak occurs at 190.3 eV due to its bonding with N in the form of BN. Like wise Nitrogen is mostly bonded to Boron as is evident from the N 1s peak occurs at 397.7 eV [80]. The C 1s peak appears at 284.9 eV due to the PVP polymeric binder. The O 1s component is located at 531.1 eV, due to the oxidation of the binder during firing. The data is quantified to get the concentration of different elements present in the coating. The individual scans of each element are shown in Figure: 3.17.

Table: 3.4 list the position of binding energy and atomic concentration corresponding to the elements B, N, C and O. The coating has 38% of B, 39% of N along with 18% of C from the binder present. 5% of oxygen is also seen in the coating due to its interaction with atmospheric oxygen during firing.

It can be seen that C and O peaks are pretty strong and then an additional N indicating that some binder is still present in the film. Therefore an additional heat treatment is needed.

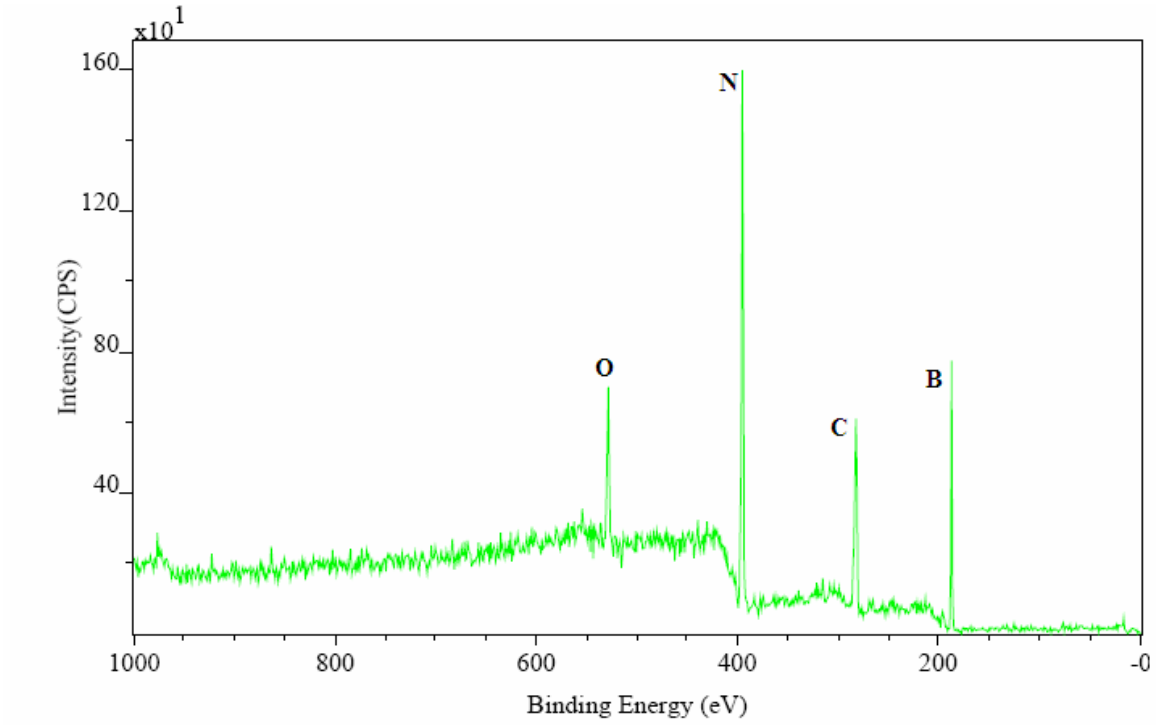

Figure 3.16: XPS Surface survey scan of PVP-BN coating fired at 200°C for 1 hour.

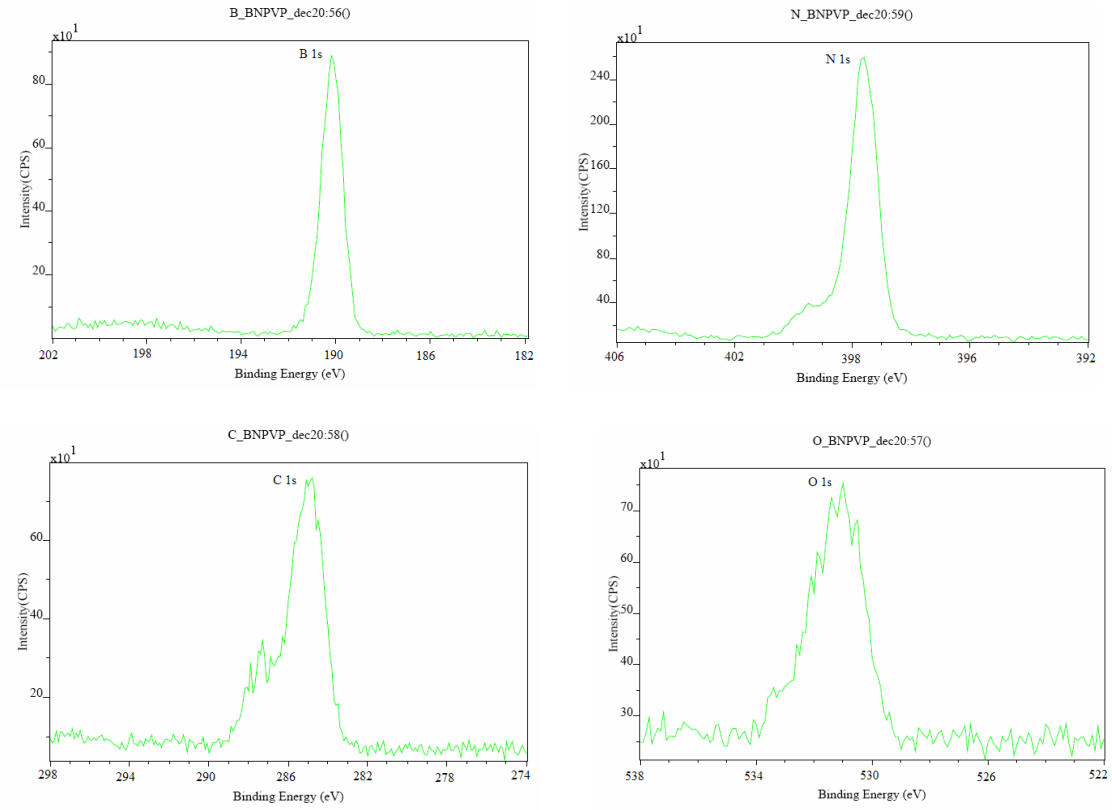

Figure 3.17: High resolution individual peaks of Boron, Nitrogen, Carbon and Oxygen of PVP-BN coating.

Peak	B.E (eV)	Atomic concentration (±3%)
B 1s	190.3	38%
N 1s	397.7	39%
C 1s	284.9	18%
O 1s	531.1	5%

Table 3.4: Quantified raw data taken from PVP-BN coatings of 0.7 and 1 BN powder (error ± 3%).

An additional firing at 600^{o}C for 30 minutes was carried on the PVP-BN coated sample to study more precisely the bonding states of B and N present in the coating. A survey XPS scan was conducted on the sample. The intense peaks seen on the spectrum are those of N 1s and B 1s at 397.9 eV and 190.3 eV respectively that corresponds to BN bonding. Trace peaks of O 1s and C 1s at 532 eV and at 284.4 eV respectively are also noticed. Table: 3.5 have the quantification data of the elements present in the coating. The atomic concentration of B is 49% while that of N is 49%. The carbon level falls to 2% from 18% while that of O to 1% from 5%. It seems that the additional heat treatment expels the carbon and oxygen present in the coating. This indicates that carbon and oxygen peaks noticed in the original coating (Figure: 3.18, Figure3.19) are that from the binder. The rise of concentrations of B and N indicates the stability of BN-coating.

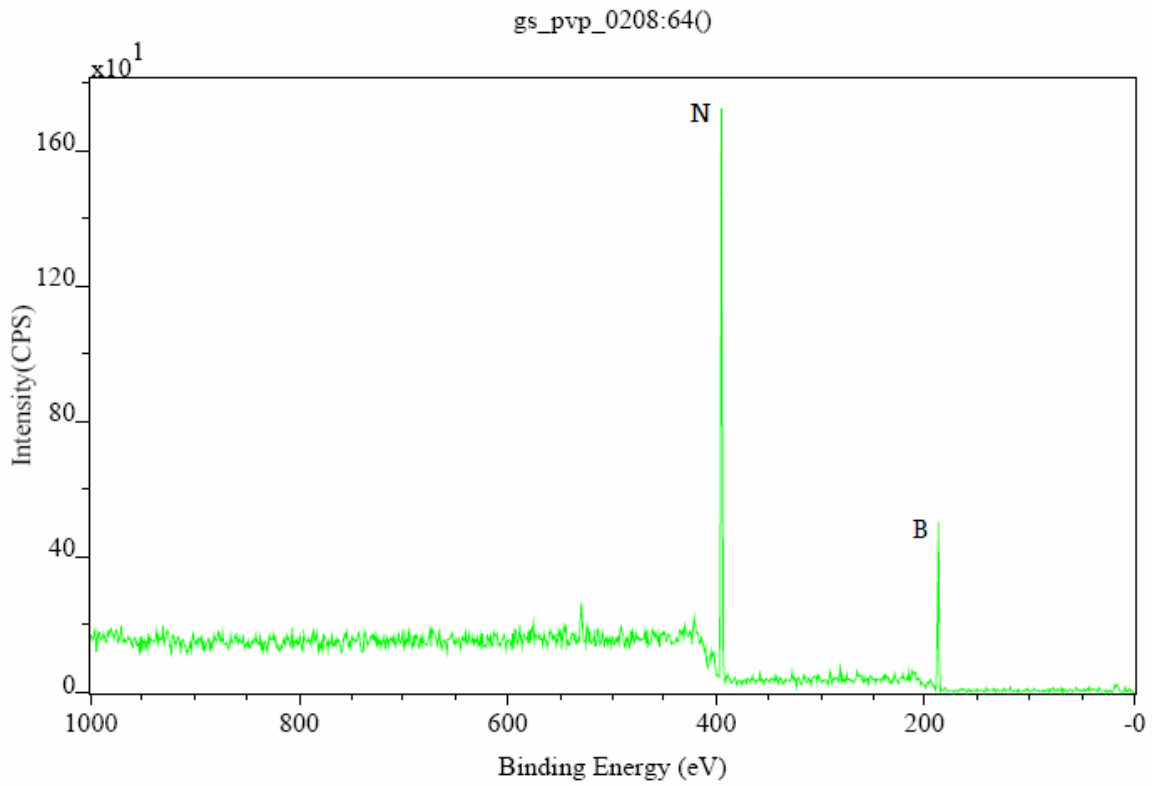

Figure 3.18: XPS survey scan of PVP-BN coatings on graphite substrate fired at 600^{0}C for 30 minutes.

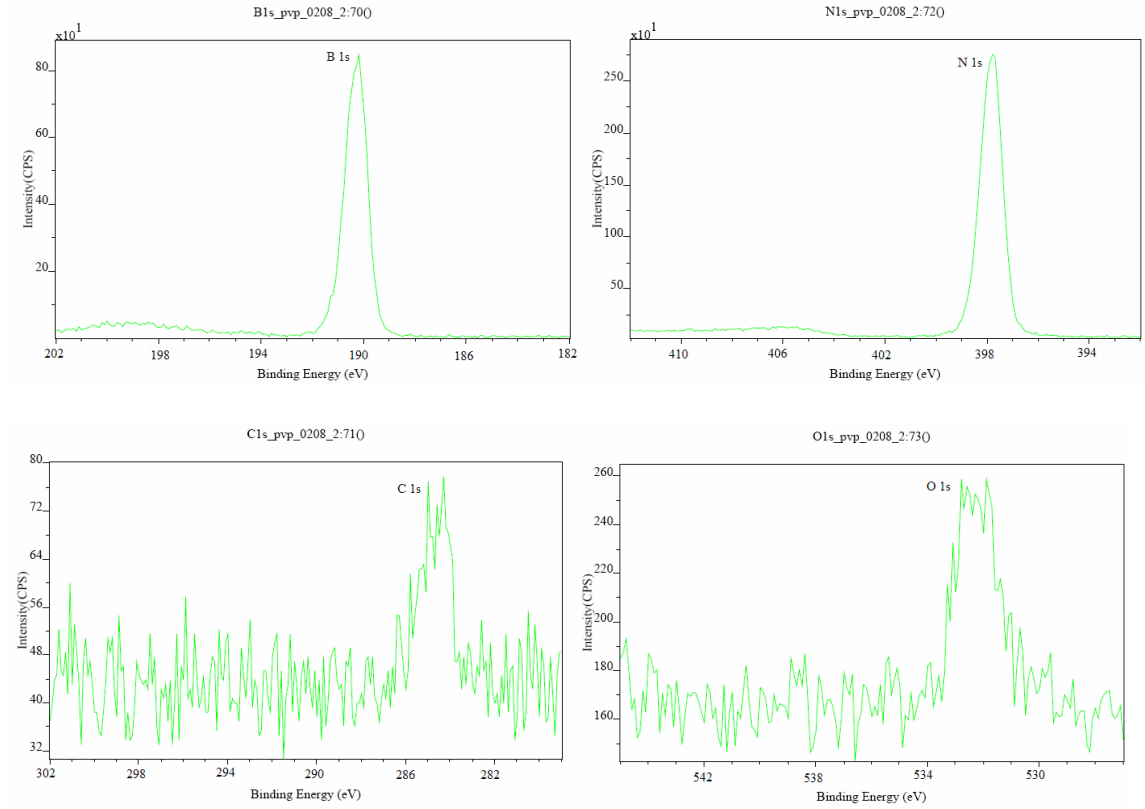

Figure 3.19: High resolution individual peaks of Boron, Nitrogen, Carbon and Oxygen of PVP-BN coating.

Peak	B.E.(eV)	Atomic concentration (± 3%)
B 1s	190.3	49%
N 1s	397.9	49%
C 1s	284.4	1%
O 1s	532	1%

Table 3.5: Quantification data for the two-step PVP-BN coating fired at 600^{o}C for 30minutes (error ± 3%).

3.4 TESTING OF PVP-BN COATINGS ON MORE ADVANCED FOAMS

3.4.1 Overview

Results of different combinations of PVP-BN coating using 1μ and 0.7μ BN particles were reported in the previous chapter. It is seen that, out of the three combinations the PVP-BN coating formed using one layer of 1μ and one layer of 0.7μ works best. This coating is now applied on different types of foams that have been optimized for different purposes. Most of the carbon foams are synthesized from a mesophase pitch. The pitch is subjected to different conditions which may be function of pressure and temperature that are proprietary. Typically, carbon foam is obtained for heat treatments at 1000^{o}C and graphite foam are obtained from heat treatments more than 2500^{o}C. If the heat treatment temperature lies between 1000^{o}C and 2500^{o}C the foam may be partially graphitized. The present Koppers foams used for testing are derived from mesophase precursor and they vary among themselves depending on the processing temperatures. The porosities of the Koppers foam used are calculated theoretically assuming a specified periodic array of interpreting spherical voids in a solid (by A.Karumuri, WSU). Assuming the models, porosity can be estimated analytically and noted on table 3.6. It must be clarified, however that this model assumes all the pores to be equally spaced having same size (Figure: 3.20). In real industrial foam this is not the case. Therefore the porosity estimates are quantitative only and quantitative may not be reliable, unless complemented with experimental measurements on porosity.

Foam	Type	cell radius	cell edge	porsity
L	carbonized	244 µm	563µm	68%
KGF	carbonized	416µm	879µm	85%
L2	carbonized	358µm	740µm	79%
L11	partially-graphitized	210µm	430µm	91%
L12	partially-graphitized	920µm	2105µm	77%
D12	graphitized	336µm	703µm	87%
L13	graphitized	253µm	542µm	80%
D1	graphitized	631µm	1286µm	92%
L14	graphitized	334µm	690µm	84%

Table 3.6: Details of the Koppers foam used for testing.

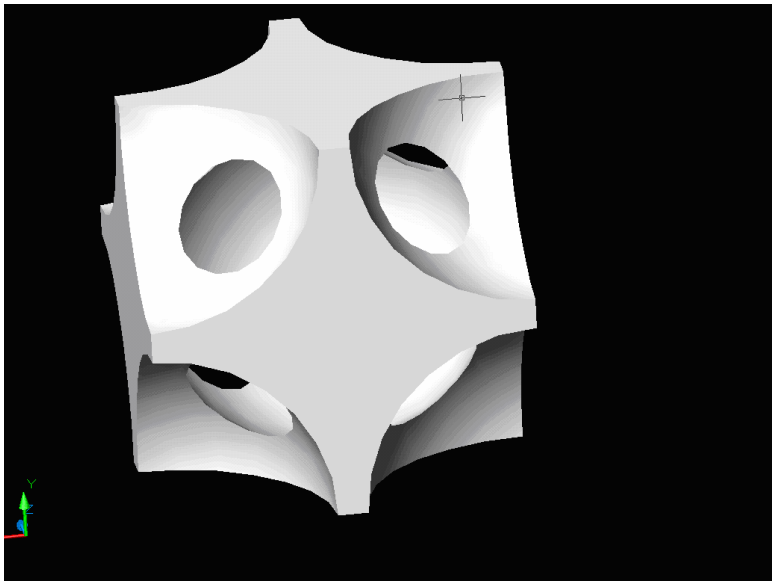

Figure 3.20: Analytical model of a unit specimen.

3.4.1 PVP-BN coating on L-Foam

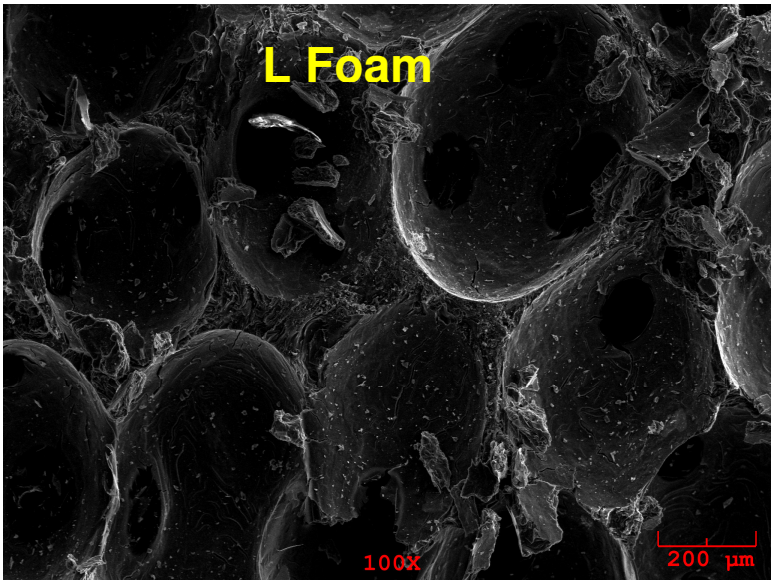

Figure 3.21: Surface morphology of Koopers L-foam.

A micrograph of the surface morphology of Koopers L-foam that is derived from 78% mesophase precursor is shown in figure 3.21. It has an average cell radius of nearly 244 µm. The L-Koopers foam was tested at 700^{o}C for 1hour, and percentage of weight loss in as received and coated is noted. Fraction of the uncoated foam left is 0.01 and fraction of BN coated foam survived is 0.26 (Table 3.7). The improvement noted due to the coating is 2600%. High improvement is noted on this foam is due to the oxidation of most of the uncoated foam.

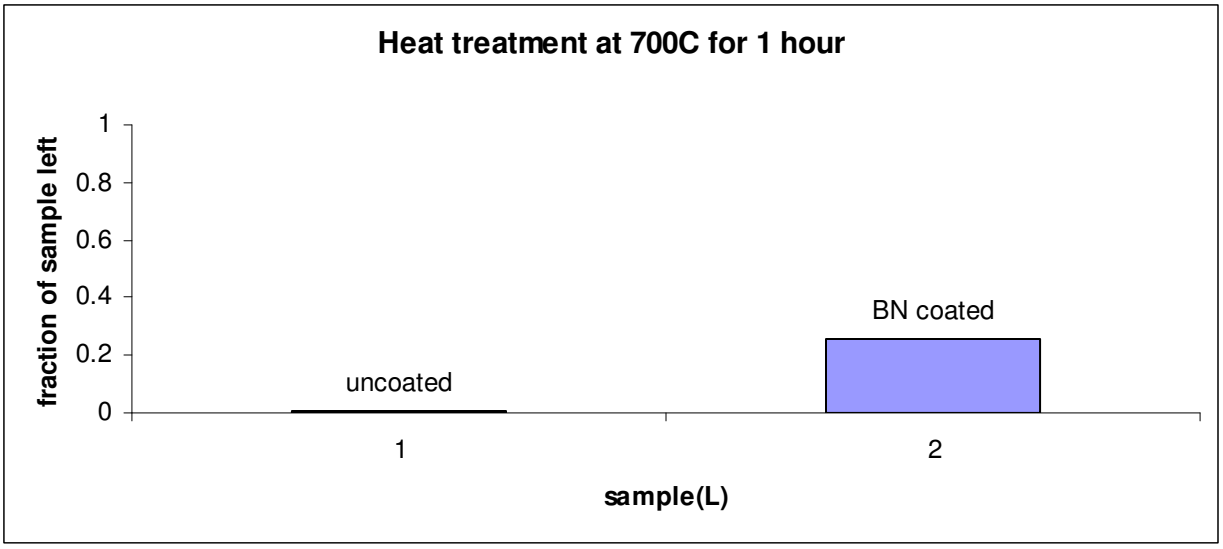

Figure 3.22: Comparison of uncoated and BN coated samples of L foam in terms of fractional amounts left.

L	Fraction of weight remaining		Improvement due to coating
	uncoated	coated	
700C for 1 hour	0.01	0.26	2500%

Table 3.7: Fractions of uncoated and BN coated samples of L foam left.

3.4.3 PVP-BN coating on KGF Foam

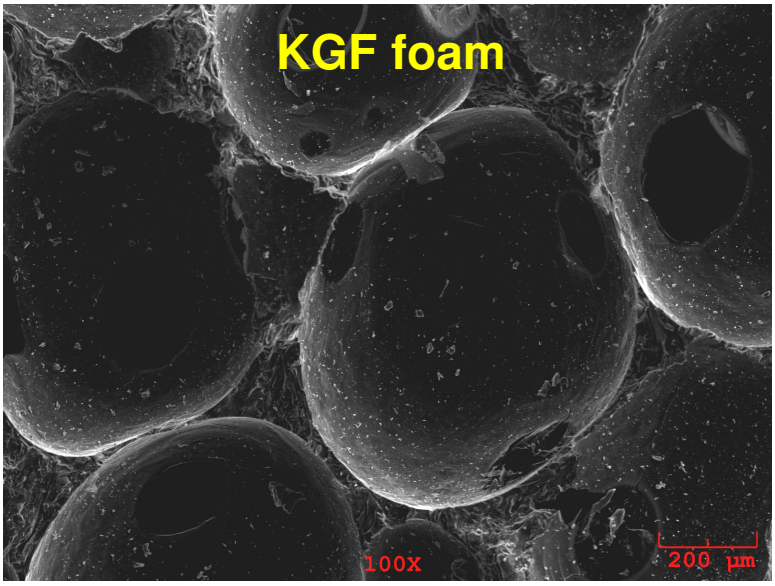

Figure 3.23: Surface morphology of Koopers KFG foam.

A micrograph of the surface texture of carbonized KFG Kopper's foam derived from 78% mesophase precursor is shown in Figure 3.23. It has an average cell radius of nearly 416µm It was heat treated at 700^{o}C for 1 hour and weight loss is measured (Figure 3.24) The fraction of uncoated sample left was 0.06 while that of PVP-BN coated sample was 0.26. The improvement due to the coating is 333% (Table 3.8).

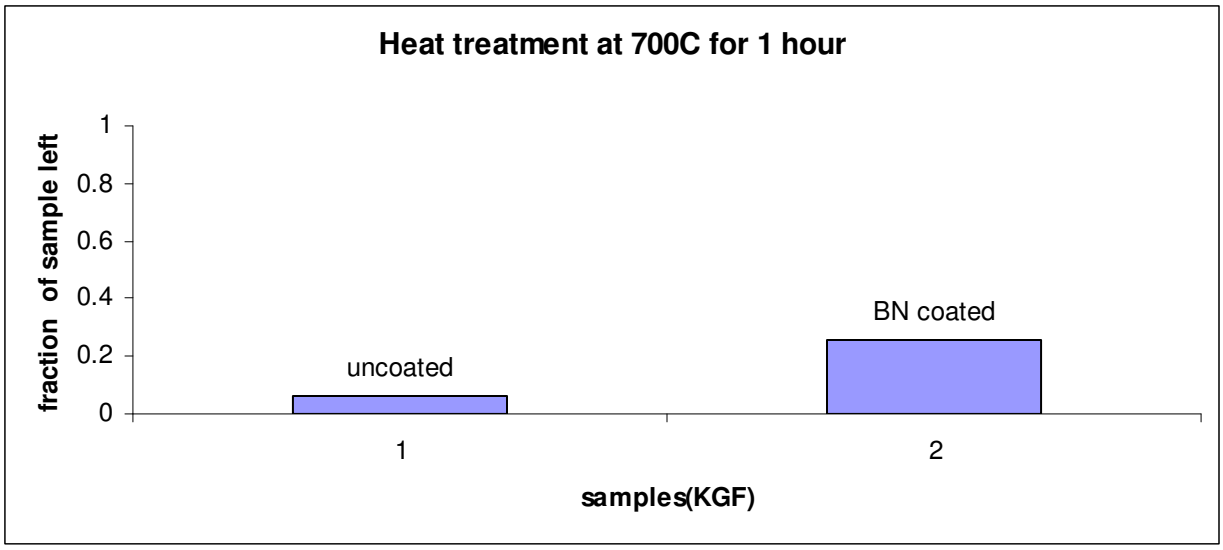

Figure 3.24: Comparison of uncoated and BN coated samples of KGF foam in terms of fractional amounts left.

KGF	Fraction of weight remaining		Improvement due to coating
	uncoated	coated	
700C for 1 hour	0.06	0.26	333%

Table 3.8: Fractions of uncoated and BN coated samples of KGF foam (error ± 5%).

3.4.4 PVP coating on Koppers L2 foam

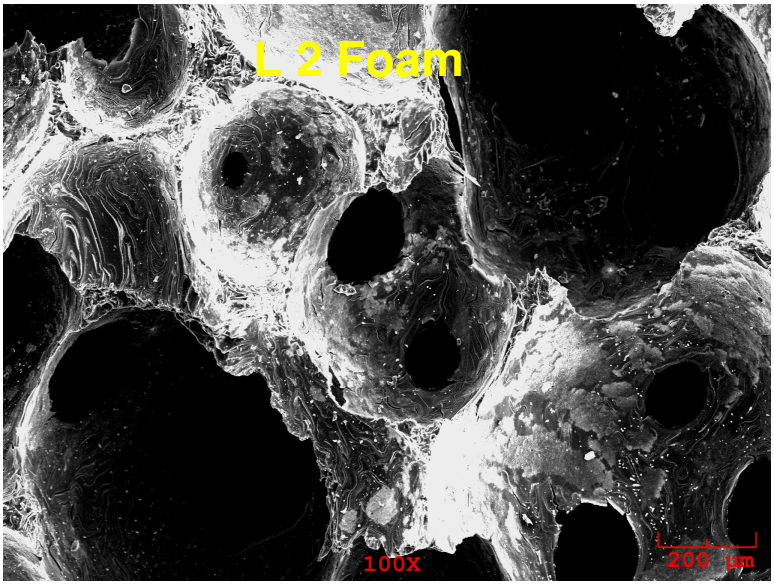

Figure 3.25: Surface topography of Koppers L2 foam.

The L2 Koppers foam is also derived from mesophase pitch and it has an average cell radius of 0.2585 mm (Figure 3.25).It is heat treated at 700^{o}C for 1 hour to check the effectiveness of the coating. At 700^{o}C for 1 hour heat treatment, weight loss of bare L2 foam is 99%, i.e. only 0.01 fraction of initial weight left (Figure 3.26). While the fractional amount of BN coated sample left was 0.31 (Table 3.9). Hence the improvement noted here was 3000% due to the coating.

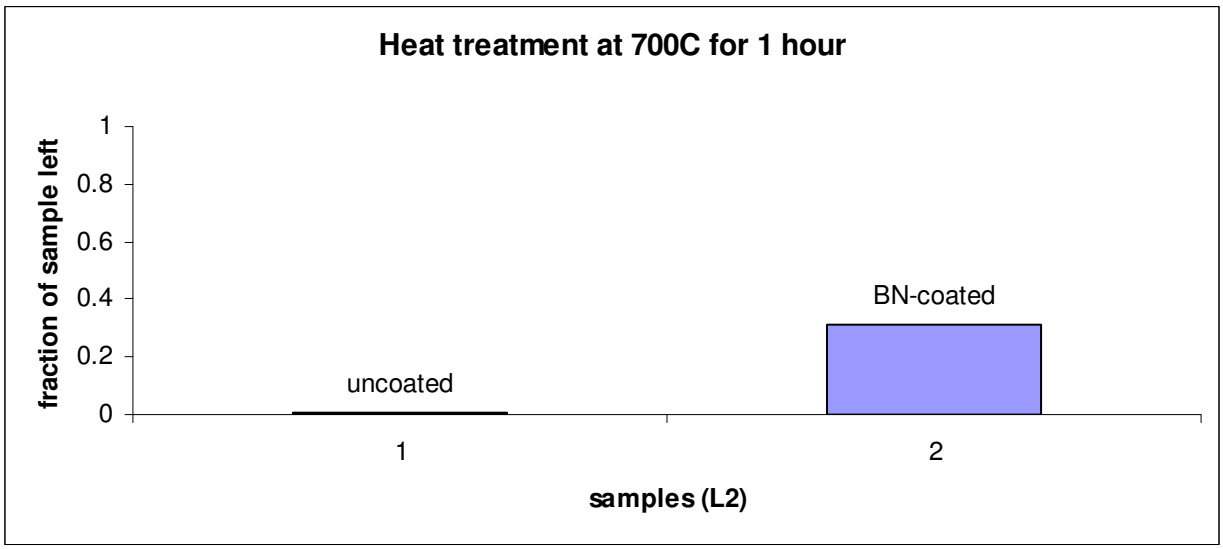

Figure 3.26: Comparison of uncoated and BN coated samples of KGF foam in terms of fractional amounts left.

L2	Fraction of weight remaining		Improvement due to coating
	uncoated	coated	
700C for 1 hour	0.01	0.31	3000%

Table 3.9: Fractions of uncoated and BN coated samples of L2 foam left (error ± 5%).

3.4.5 PVP coating L11 foam

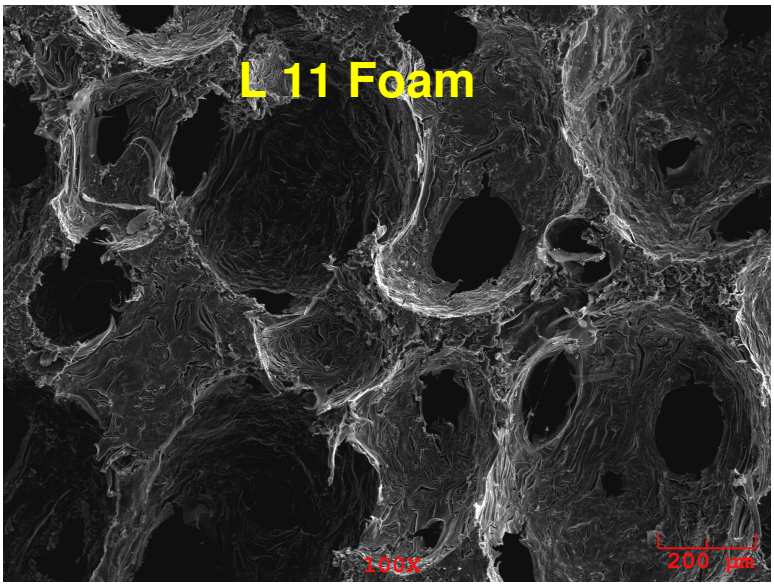

Figure 3.27: Surface topology of Koppers L11 foam.

A micrograph of the surface morphology of the L11 foam is shown in Figure 3.27 and this foam is also derived from mesophase pitch. It has a cell radius of approximately 210µm. L11 foam is tested at 700°C for 1 hour. The fractional amount of as-received sample left was 0.69% while that of BN coated sample left was 0.84 (Figure 3.28). The survivability improved to 22% due to the coating (Table 3.10).

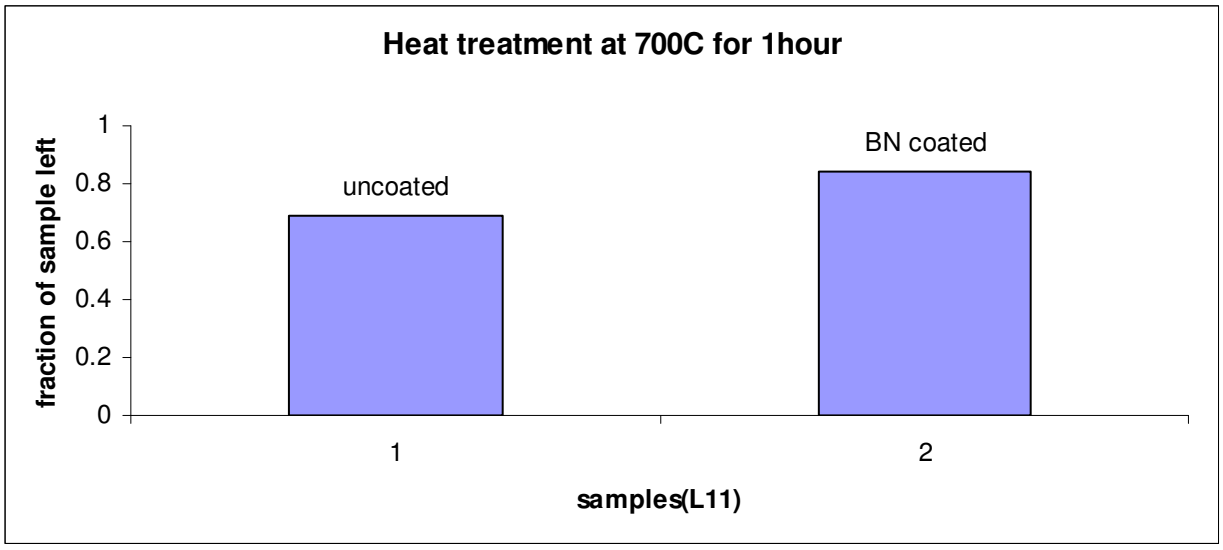

Figure 3.28: Comparison of weight loss of as-received and PVP_BN L11 foam at 700^{o}C for 1 hour.

L11	Fraction of weight remaining		Improvement due to coating
	uncoated	coated	
700C for 1 hour	0.69	0.84	22%

Table 3.10: Fractions of uncoated and BN coated samples of L11 foam left (error ± 5%).

3.4.6 PVP-BN coating on L12

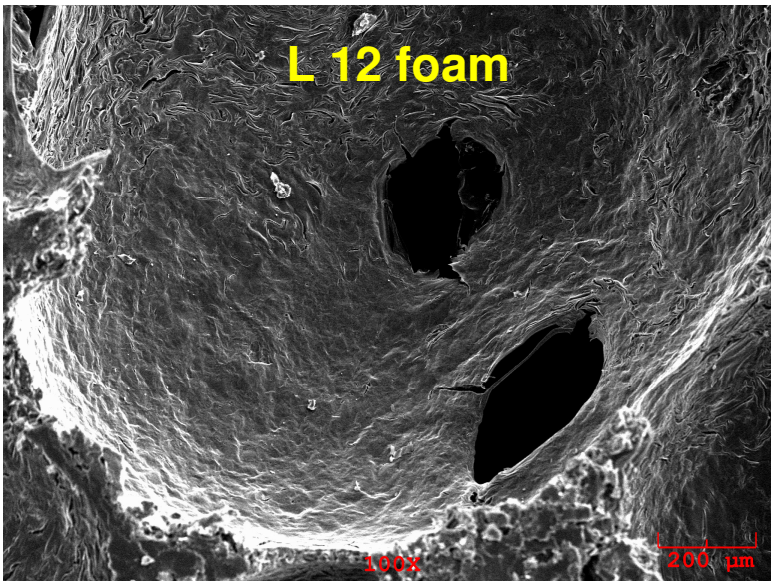

Figure 3.29: Surface texture of Koppers L12 foam.

The Koppers L12 foam was derived based on mesophase pitch. It has cell radius nearly 0.92mm (Figure 3.39). It was heat treated at 700^{o}C for 1 hour. Amount of uncoated sample left was 0.72. Amount of PVP-BN coated sample left was 0.92 (Figure 3.30). The improvement noted here due to coating was 27% (Table 3.11).

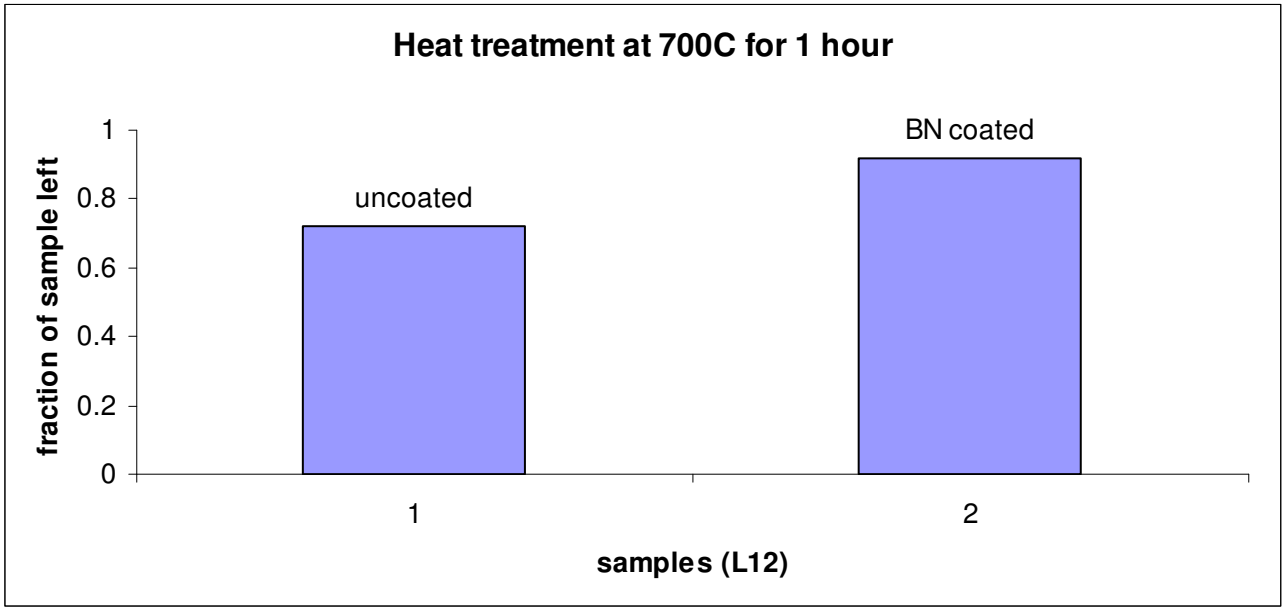

Figure 3.30: Comparison of uncoated and BN coated samples of L12 foam in terms of fractional amounts left.

L12	Fraction of weight remaining		Improvement due to coating
	uncoated	coated	
700C for 1 hour	0.72	0.92	28%

Table 3.11: Fractions of uncoated and BN coated samples of L11 foam left (error ± 5%).

3.4.7 PVP-BN coating on L13 foam

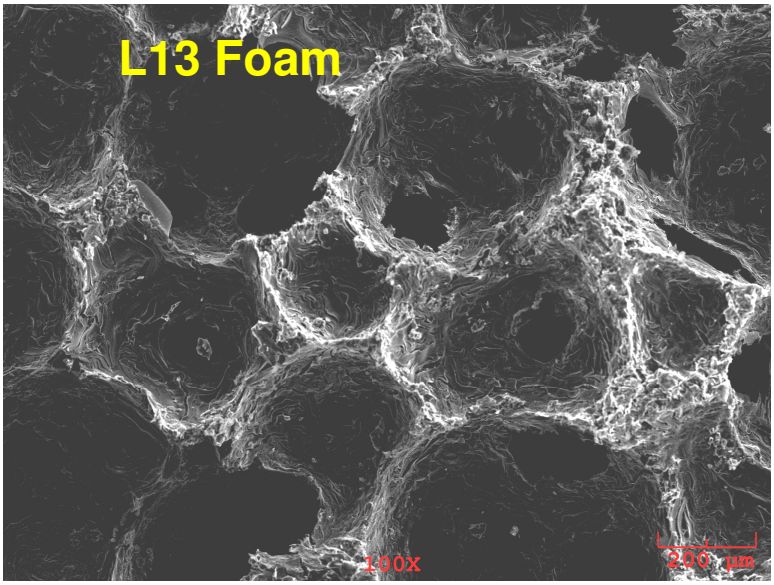

Figure 3.31: Surface topography of L13 foam.

L13 foam was also derived from mesophase pitch has a cell radius 253µm. The foam is heat treated at 700^{o}C for 1 hour and the weight loss was measured. The fraction of uncoated L13 left was 0.84 while that of coated one left was 0.9. Improvement noted due to the BN coating was 7%. There is not significant change in weight loss of L13 at 700^{o}C that may be due to graphitization of the foam. So the foam was again heat treated at 800^{o}C for 1 hour. At 800^{o}C the uncoated foam retains 0.18 fraction of initial weight while PVP-BN coated retains 0.78 of its weight (Table 3.12). Now the improvement noted was 333% which shows that PVP-BN coating works effectively in improving the oxidation resistance of the graphitized L13 foam. There is a significant finding that indicates that this coating developed using a simple environmentally benign method can have good practical use at high temperature for the so called high performance graphite foam.

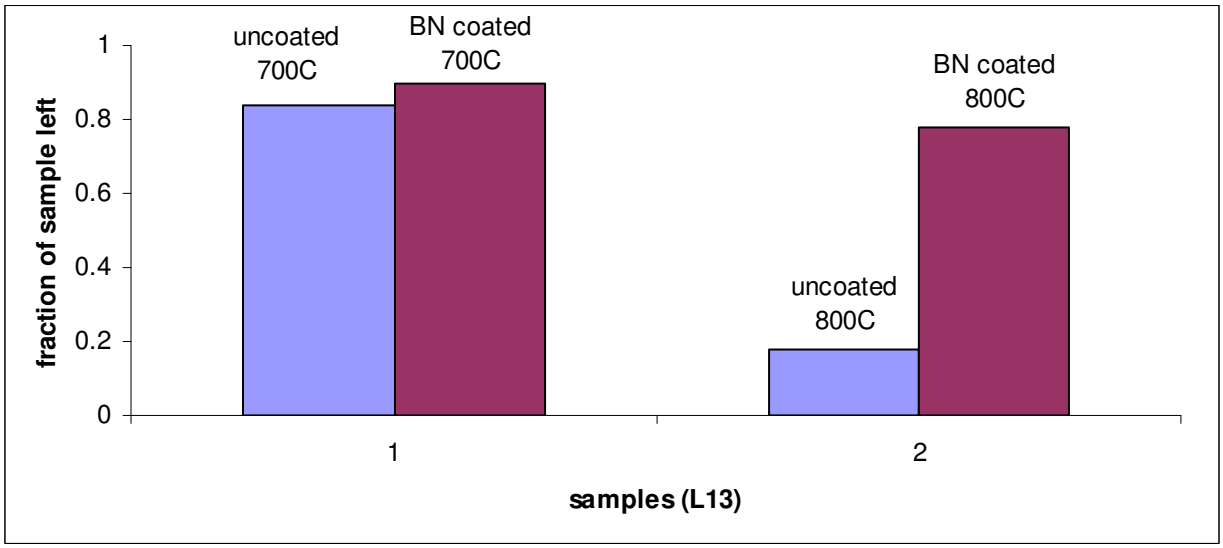

Figure 3.32: Comparison of uncoated and BN coated samples of L12 foam in terms of fractional amounts left.

L13	Fraction of weight remaining		Improvement due to coating
	uncoated	coated	
700C for 1 hour	0.84	0.90	7%
800C for 1 hour	0.18	0.78	333%

Table 3.12: Fractions of uncoated and BN coated samples of L13 foam left (error ± 5%).

3.4.8 PVP-BN coating on D1 foam

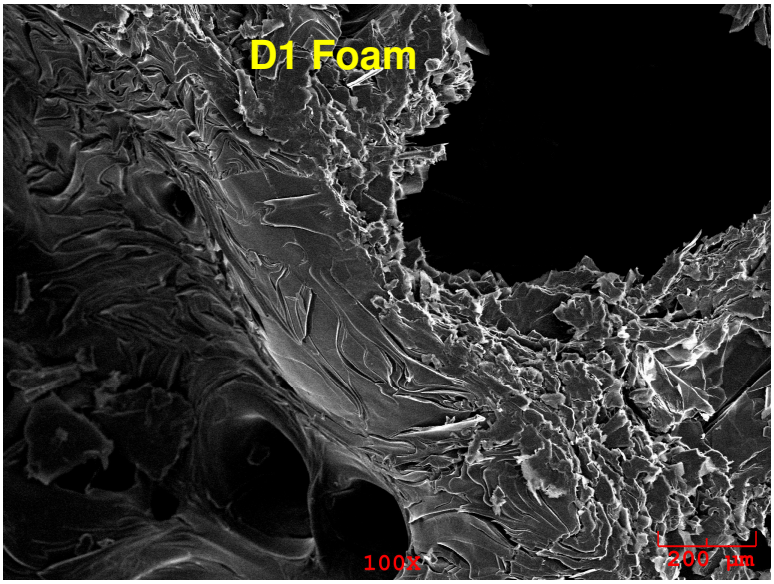

Figure 3.33: Surface morphology of D1 foam.

The D1 Koppers foam is graphite foam with a cell radius of about 631µm (based on analytical calculations).This foam was heat treated at 700^{o}C for 1hour and the fraction weight of sample left was 0.89. The fraction of the PVP-BN coated sample survived was 0.92. The coating improved the performance to 3%. At 800^{o}C heat treatment, fractional weight of uncoated D1 foam retained was 0.2 while that of PVP-BN coated on was 0.87 (Table 3.13). The survivability improved to 335%, which is again significant improvement due to coating.

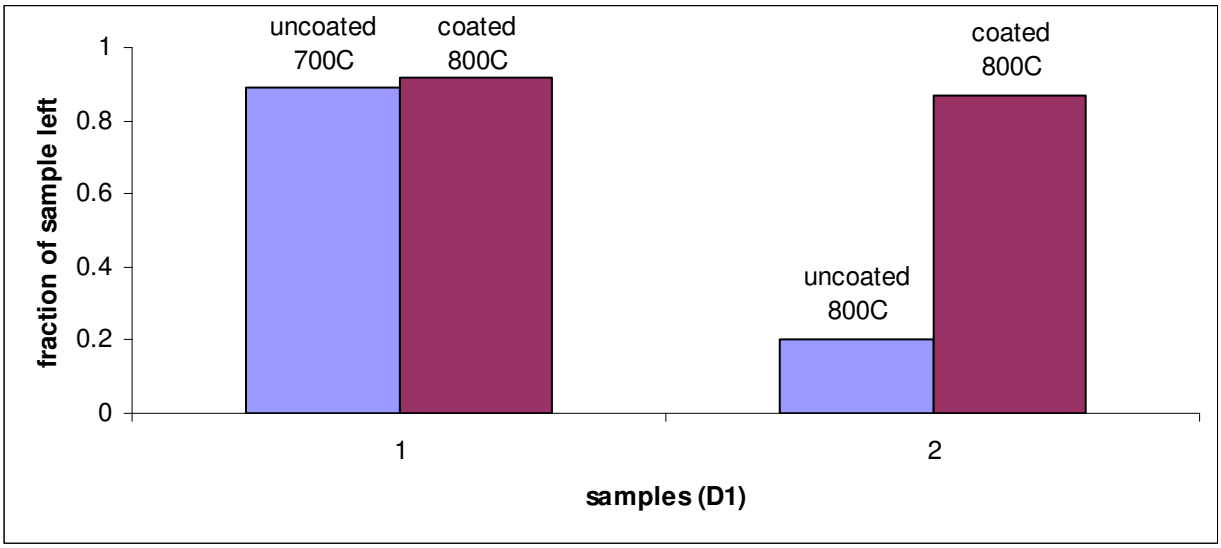

Figure 3.34: Comparison of uncoated and BN coated samples of D1 foam in terms of fractional amounts left.

D1	Fraction of weight remaining		Improvement due to coating
	uncoated	coated	
700C for 1 hour	0.89	0.92	3%
800C for 1 hour	0.2	0.87	335%

Table 3.13: Fractions of uncoated and BN coated samples of D1 foam left (error ± 5%).

3.4.9 PVP-BN coatings on L14 foam

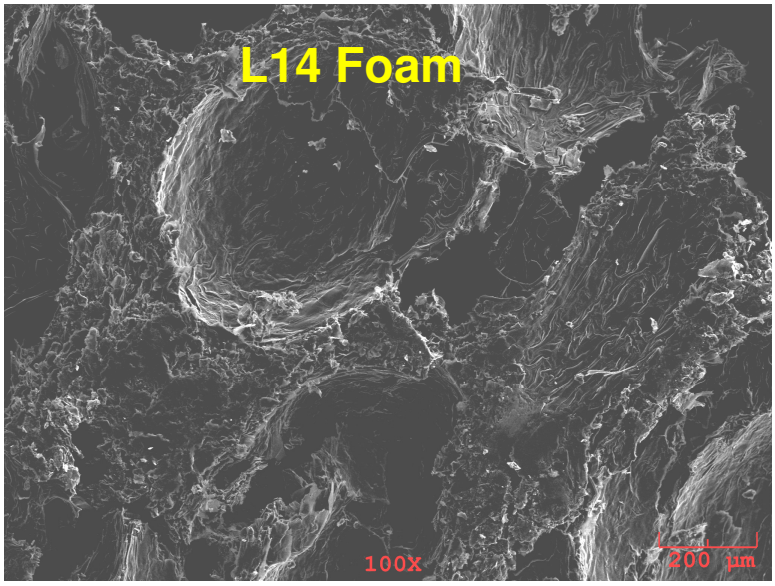

Figure 3.35: Surface texture of Koppers L14 foam.

L14 foam is mesophase precursor-based Koppers foam having an average cell radius of about 334.µm. When the foam was heat treated at 700^{o}C for 1 hour, 0.78 and 0.9 fraction of uncoated and PVP-BN coated foams were left respectively. When heat treated at 800^{o}C for 1 hour, fraction of the uncoated foam left was 0.61 while PVP-BN coated L14 retains 0.8 fraction of its weight (Table 3.14).The coating increased the survivability at 800^{o}C to 31%.

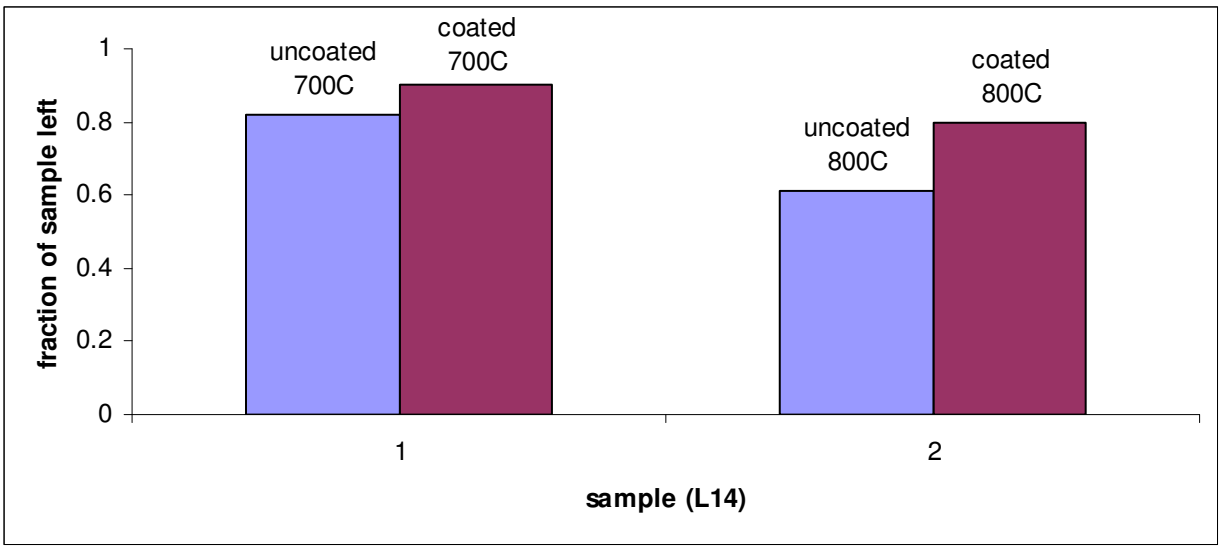

Figure 3.36: Comparison of uncoated and BN coated samples of L14 foam in terms of fractional amounts left.

L14	Fraction of weight remaining		Improvement due to coating
	uncoated	coated	
700C for 1 hour	0.82	0.9	10%
800C for 1 hour	0.61	0.8	31%

Table 3.14: Fractions of uncoated and BN coated samples of L14 foam left (error ± 5%).

3.4.10 PVP-BN coating on D12 foam

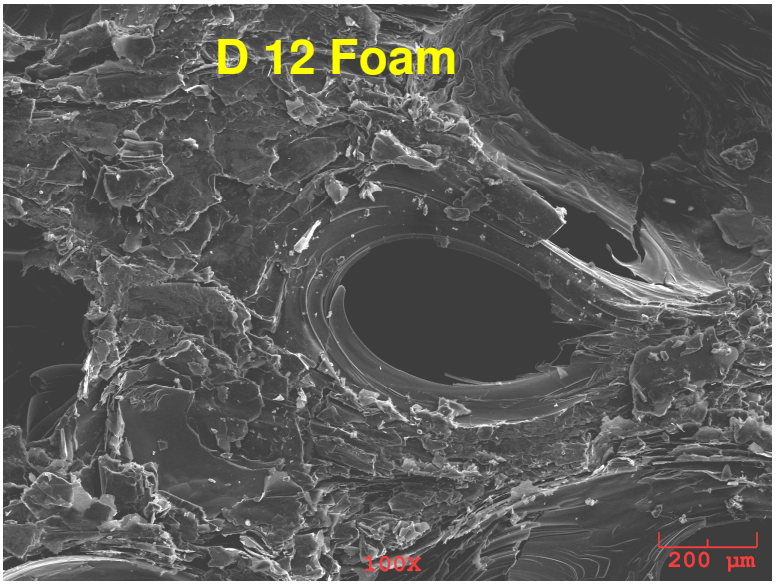

Figure 3.37: Surface morphology of Koppers D12 foam.

The D12 is a Koppers graphitized foam having a cell radius of 336µm. For 1 hour heat treatment at 700^{o}C the fraction of the foam left was 0.87 while in the case of PVP-BN coated foam was 0.91. At 800^{o}C for 1 hour heat treatment the bare foam left was 0.09 fraction of its initial weight while 0.24 fraction of the PVP-BN coated foam was left (Table 3.15). The improvement noted due to the coating at 800^{o}C is 167%.

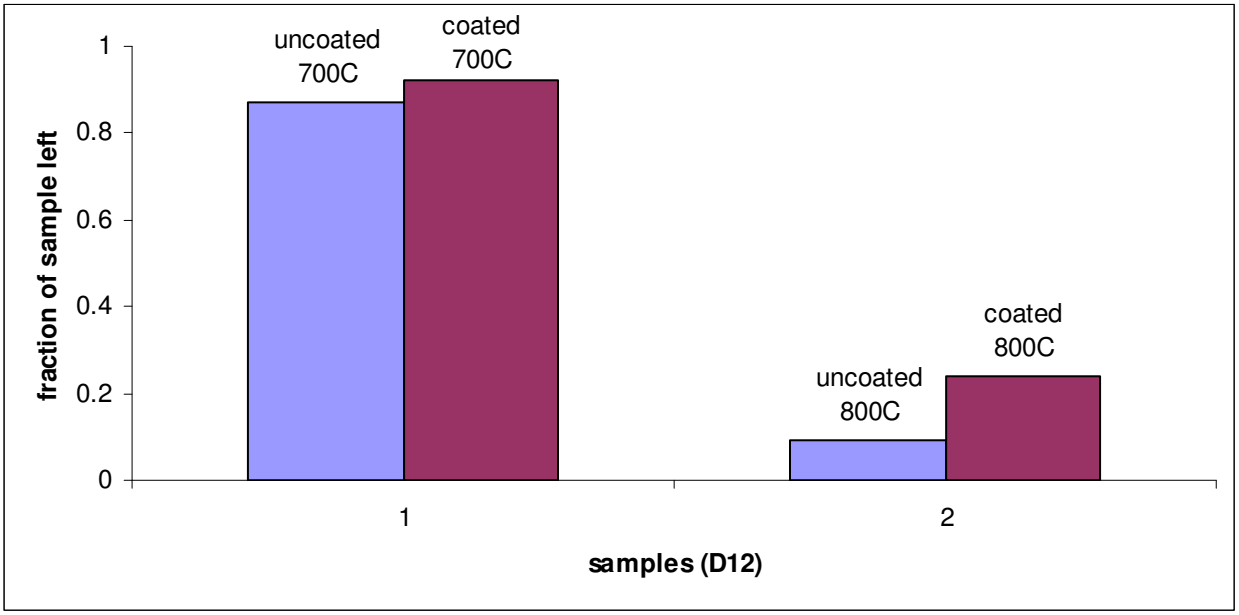

Figure 3.38: Comparison of uncoated and BN coated samples of L14 foam in terms of fractional amounts left.

D12	Fraction of weight remaining		Improvement due to coating
	uncoated	coated	
700C for 1 hour	0.87	0.91	6%
800C for 1 hour	0.09	0.24	167%

Table 3.15: Fractions of uncoated and BN coated samples of L14 foam left (error ± 5%).

3.4.11 Variation of level of protection

As per the above observations it may be noted that PVP-BN coatings improve the resistance against of all kinds of Koppers foams but the extent of protection seem to vary from structure to structure.

The performance of PVP-BN coating can depend on various factors. For carbonized foams like L, KGF, L2 foams the weight loss is significant at 700^{o}C heat treatment for 1hour is more. With PVP-BN coating on L, and L2 foams that have retain nearly same weight have showed the similar improvement (Table 3.16). The fractional weight retained by bare L11 and L12 foams is 0.69 and 0.72 which is less than that of L, KGF, and L2 foam is due to certain amount of graphitization. When PVP-BN coating is applied on L11 and L12 the improvement noted is 21% and 27% respectively. For heat treatment at 700C for 1 hour, graphite foams D1, L13, L14 and D12 retains the most of the foam for heat treatment.

At 800^{o}C the PVP-BN coatings the improvement noted for L13, D1, D12 and L14 was 333%, 334%, 167% and 31% respectively. It appears that L14 is more graphitized and more stable as it retains more weight compared to that of L13, D1 and D12. L13, D1 and D12 were compared further because they had comparable weight loss but different improvement with coating. The improvement shown due to the coating for L13 and D1 is more than that of D12 (Table 3.16). These edges were carefully observed are observed using SEM at higher magnification. The cell wall dendrites of D1, L13 exhibit rough

flake-like structure show significant improvement of more than 300% in comparison to D12 where there is only 167% improvement. This is an indication that the surface morphology of the cell walls also plays a role in performance of this liquid based coating. The improvement in rough edges may be due to increased binding between the coating and substrate.

Foam	Uncoated	PVN-BN coated	Improvement (%) (error ± 5%)
L	0.01	0.26	2500%
KGF	0.06	0.26	333%
L2	0.01	0.31	3000%
L11	0.69	0.84	22%
L12	0.82	0.92	27%

Table 3.16: Summary of results on carbon foams.

Foam	700C for 1 hour (error ± 5%)			800C for 1 hour (error ± 5%)		
	uncoated	coated	Improvement	uncoated	coated	Improvement
L13	0.84	0.09	7%	0.18	0.78	333%
D1	0.89	0.92	3%	0.2	0.87	335%
D12	0.87	0.91	6%	0.09	0.24	167%

Table 3.17: Summary of results on graphite foams.

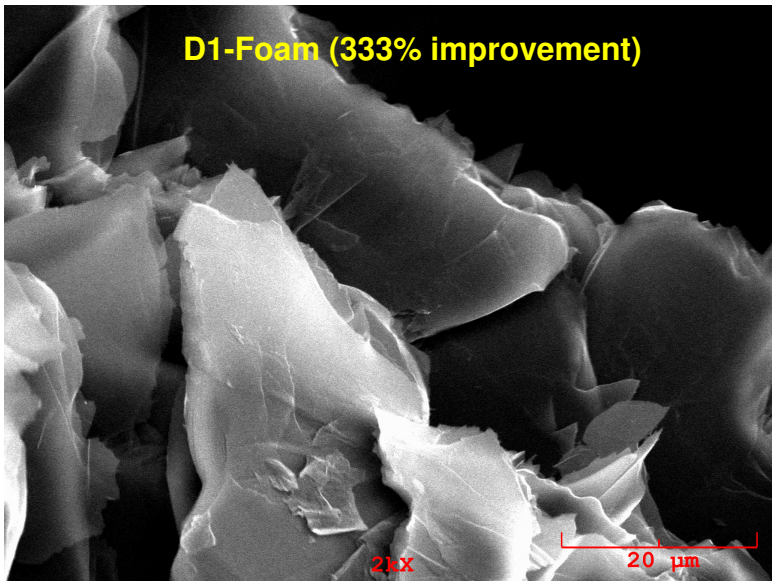

Figure 3.39: Surface morphology of bare D1 foam.

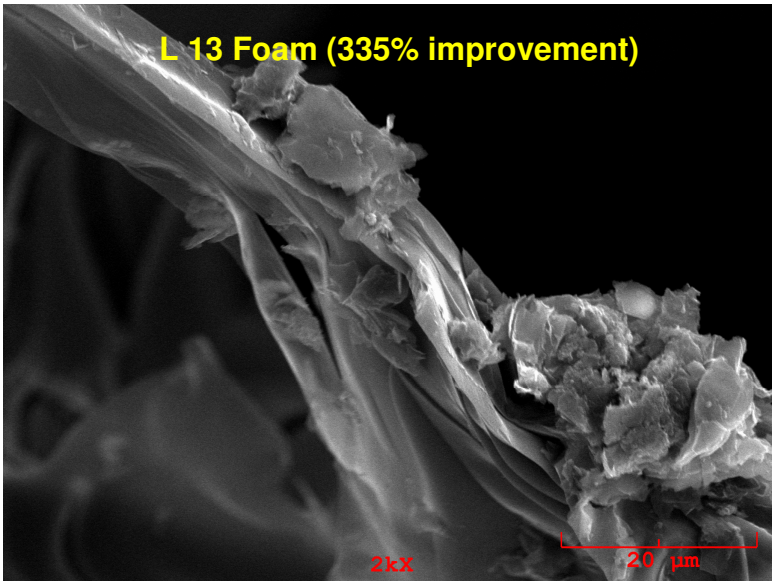

Figure 3.40: Surface morphology of bare L13 foam.

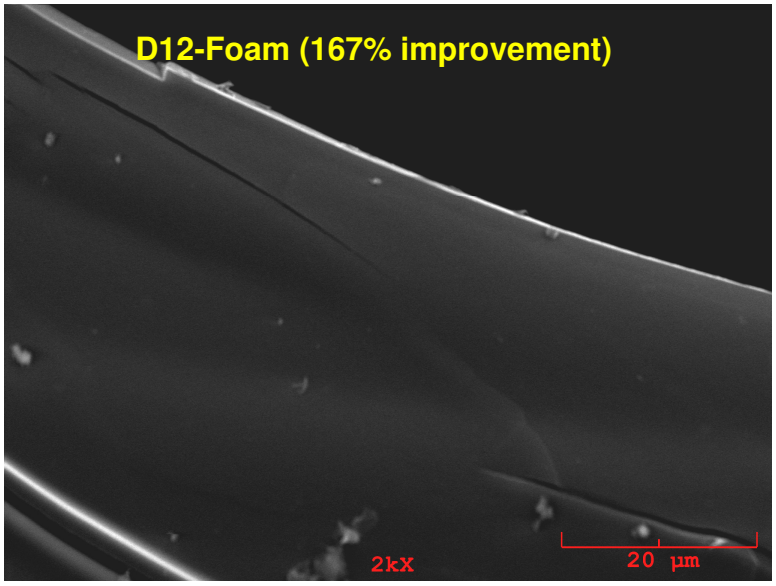

Figure 3.41: Surface morphology of bare D12 foam.

4 SUMMARY & FUTURE WORK

4.1 SUMMARY

The oxidation resistance of the carbon foams is improved by PVP-BN coatings. Different coating combinations of PVP-BN coating using 0.7μ and 1μ BN particles are studied. The surface morphology of the coatings is observed using SEM and FESEM. The surface micrograph of the coating formed using 1μ BN particles only, show that the coating comprised of clusters of BN particles. The micrograph of coating formed using 0.7μ BN particles consisted of smaller particles compared to that of 1μ coating. The best performing coating is a two layer one with 1μ BN layer followed by 0.7μ BN layer. This coating combination is selected and studied over different types of carbon foams. The coating chemistry is analyzed using X-ray Photo-electron Spectroscopy. The XPS studies show that after heat treatment at 200^{o}C there is essentially BN with some organic binder. and after 600^{o}C it is pure chemical BN.

The PVP-BN coatings were tested on a variety of foam ranging from carbonized to graphitized structures that are optimized by industry for different applications. The results indicate that coating improves all foams to various degrees. The overall improvements of the PVP-BN coating may depend on surface morphology of the cell walls. In graphite foams like D1 and L13 the surface rough surface dendrites show a more improved performance than that of D12 which have smooth dendrites under similar conditions.

4.2 FUTURE WORK

- In this study, a two layer PVP-BN coating using two sizes of BN particles was used. These coatings can be further improved by carefully varying solution properties such as binder and particle size distribution.
- Carbon foams can be subjected to multi-layer coatings using different types of material. The hierarchy at which coating material used may depend on its properties such as coefficient of thermal expansion, chemical stability thermal conductivity.
- There is a scope for tailoring the properties of the carbon foam by using careful selection of coating materials by using ceramic materials such as SiC, Al_2O_3 and metallic materials like Al, Ni etc. This work is to be continued in this group.

5 REFERENCES

1 "Surface Engineering of Metals Principles, Equipment, Technologies", T.Burakowski, T.Wierzchon CRC Press, (1999).

2 "On the corrosion resistance of the Delhi iron Pillar" R. Balasubramaniam, Corrosion Science 42, 2103-2129, (2000).

3 "Principles of electroplating and electroforming (electrotyping)" Blum William, New York, McGraw-Hill, (1949).

4 "Surface engineering past present and future" Bell T , Surface Eng, Vol 6, 31-40, (1990).

5 "Hand book of Chemical vapor deposition Principles, Technology and Application" Hugh O. Pierson, Noyes Publications, (1992).

6 "Ceramic Films and Coating" John Wachtman and Richard A. Haber, Noyes Publications, (1992)

7 "Surface engineering & heat treatment past, present and future", P.H.Morton, The Institute of Metals, (1991).

8 "High performance ceramic films and coating" P.Vincenzini, Material science monographs, 67, (1991).

9 "Chemical Vapor Deposition", Jong Park, Surface engineering series, ASM international, (2001).

10 "Surface Engineering for manufacturing applications", Steve J Bull, Material Research Society, symposium proceedings, vol 890, (2005).

11 "Oxidation protection of graphite foams" James Klett, Rick Lowden, April McMillan Proceedings of the 2nd World Conference on Carbon, July 13-18, Lexington, Kentucky, USA (2001).

12 "Surface modification of graphitic foam" S M Mukhopadhyay, R V Pulikollu, E Ripberger and A J Roy, J of applied physics, Vol 93, 878-882, (2003)

13 "Structural investigation of graphitic foam" S.M Mukhopadhyay, N. Mahadev, and P. Joshi, J of applied physics, 3415-3420, (2002).

14 " Thin Films for Coating Nanomaterials", S.M. Mukhopadhyay, Pratik P. Joshi, Rajasekhar V. Pulikollu, Tsinghua Science and Technology, China, Vol. 10, No.6, 277 – 287, (2005)

15 "Nano-coating on carbon structures for interfacial modification", PhD dissertation, RV Pulikollu Wright State University, (2005)

16 "Oxidation protection of graphite by BN coatings" A Nechepurenko and S Samuni, Journal of Solid State chemistry,162-164, (2000)

17 "Surface engineering of metals" T Burakowski, T Wierzchon, CRC press (1999).

18 "A high temperature oxidation resistant coating, for graphite, prepared by atmospheric pressure chemical vapor deposition" N Bahlawane, Thin solid films 298-303, (2001).

19 "Applied material science" Deborah D.L.Chung, CRC Press, (2000).

20 "Cellular ceramics" Michael Scheffler and Paolo Colombo, Wiley –VCH, (2004).

21 "Coatings with particulate dispersions for high temperature oxidation protection of carbon and c/c composite" A Joshi, J S Lee, Composites 181-189, (1997).

22 “Micro structural evaluations of Si-Hf-Cr fused slurry coating for oxidation protection of graphite” HS Hu, A Joshi and J S Lee, Journal of vacuum science and technology, Vol 9 1535-1538, (1991).

23 “Oxidation resistant SiC coating for graphite materials” Q Zhu, X Qiu, C Ma, Carbon, 1475-1484, (1999).

24 “Growth of SiC thin films on graphite for oxidation protective coating” J H Boo, M C Kim, S B Lee, S J Park, J G Han, Journal of American vacuum science and technology, Vol 18 1713-1717, (2000).

25 “Single-crystalline, epitaxial cubic SiC films grown on (100) Si at 750 °C by chemical vapor deposition” I Golecki, F Reidinger, J Marti, Applied physics letters, Vol 60, 1703-1705, (1992).

26 “Epitaxial growth of 3CSiC on Si (111) from hexamethyldisilane” CH Wu, C Jacob et al, J of Crystal Growth, Vol 158 480-490, (1996).

27 “Si-C /B containing coatings for the oxidation protection of graphite”, J W Fergus and W L Worrell, Carbon, Vol33, 537-543, (1995).

28 “Oxidation protection of carbon materials by acid phosphate impregnation” W Lu, DDL Chung Carbon, Vol 40 1249-1254, (2001).

29 “The influence of aluminum phosphates on graphite oxidation” Christopher R. Maier, Linda E. Jones, Carbon, Vol 43, 2272–2276, (2005).

30 “Oxidation of carbons in the presence of chlorine” J Gonzalez, M C Ruiz, A. Bohe, D Pasquevich, Carbon, Vol 37 1979–1988, (1999).

31 “Formation of oxidation resistant graphite flakes by ultra thin silicone coating” H Konno, T Kinomura, H Habazaki, M Aramata, Surface & Coatings Technology Vol 194,24– 30, (2005).

32 “Heavy oil sorption using exfoliated graphite new application of exfoliated graphite to protect heavy oil” M Toyoda, M Inagaki, Carbon, Vol 38, 199–210, (2000).

33 “Principles of extractive metallurgy” Habashi, Fathi Gordon and Breach science publisher, NY (1980).

34 “The inhibiting effect of chlorine or carbon tetrachloride on graphite oxidation” R. C. Asher and T. B. A. Kirstein J of nuclear materials, 344-346, (1968).

35 “Multilayered coatings for protecting carbon-carbon composites from oxidation”, M Guo, K Shen, Y Zheng , Carbon, Vol 4 449-453, (1995).

36 “Multi layer coatings on CFC composites for high temperature applications, V Wunder, N Popovska, A Wegner, G Emig, W Arnold, Surface and coating technology, 329-32, (1998).

37 “Carbon-boronsilicide and oxide composites coatings on carbon materials” V I Zmii, G N Kartmazov, N F Kartsev, S G Rudenkii and N S Poltavtsev, Powder Metallurgy and Metal Ceramics, Vol 45, 124-128 (2006).

38 “Protective multilayer coating for carbon-carbon composites” C Fredrich, R Gadow, M Speicher, Surface and Coating Technology, 405-411, (2002).

39 “Protective coatings for carbon fibers” N.I. Baklanova, T M. Zima, A T Titov, N V Isaeva, D V Grashchenkov and S S Solntsev, Inorganic Materials, Vol 42, 744-749, (2006).

40 “Multi-layer Coating for carbon-carbon composites” T.Morimoto, Y Ogura, M Kondo and T Ueda, Carbon, Vol 33, 351-357, (1995).

41 “Anti Oxidation of carbon-carbon composites by SiC concentration gradient and zircon over coating” O Yamamoto, T Sasamoto and M Inagak, carbon, Vol 33, 359-365, (1995).

42 “CVD and CVR Silicon based functionally gradient coatings on C-C composites” W Kowbell, J C Withers, Carbon, Vol 33, 415-426, (1995).

43 “Formation of a functionally gradient (SiC+SiC)/C layer for the oxidation protection of carbon-carbon composites” Y Zhu, S Ohtani, Y Sato, N Iwamoto, Carbon, Vol 37, 1417-1423, (1999).

44 “Investigation on the properties of carbon fiber with C-Si functionally gradient coating” S Chu, H Wang, R Wu, Surface and Coating Technology, Vol88, 38-43, (1997).

45 “Particulate containing glass sealants for carbon-carbon composites”, F.J.Buchanan, J A Little, Carbon, Vol 33, 491-497, (1997).

46 “Hybrid PACVD SiC/CVD Si_3N_4 multi layer coating for oxidation protection of composites” H T Tsou, W Kowbell, Carbon, Vol 33, 1279-1288, (1995).

47 “Hybrid PACVD B_4C/CVD Si_3N_4 multi layer coating for oxidation protection of composites” H T Tsou, W Kowbell, Carbon, Vol 33, 1289-1292, (1995).

48 “Formation and oxidation resistance of the coating formed on carbon material composed of B4C-SiC powders”, K.Kobayashi, K Maeda, H Sano, Y Uchiyama, Carbon, Vol 33,397-403, (1995).

49 "Oxidation resistant material for carbon/ carbon composites by the Sol-Gel process", V.K.Parashar, V Raman, O P Bahl, J of Material Science Letters 16, 479-481, (1997).

50 "Preparation and characterization of SiC coated C/C composites using pulse layer chemical vapor deposition (pulse-CVD)", A Saka, N Kitamori, K Nishi, S Motojima, Material letters, 61-64, (1995).

51 "Oxidation Resistant carbon-carbon composite up to 1700^{o}C", T L Dhami et al., Carbon, Vol 33, 479-490, (1995).

52 "Synthetic routes to Boron Nitride", R T Paine, C K Narula, Chem Rev, 90, 73-91, (1990).

53 "Ceramic precursor technology and its applications" C K Narula, M Dekker Inc, (1995).

54 "BN coatings on steel and graphite produced with low pressure RF plasma", O Gafri, A Grill, D Itzhak, Thin solid Films, 72, 523-527, (1980).

55 "Synthesis of Boron Nitride thin films", D R McKenzie, Surface and Coating Technology, 255-262 (1996).

56 "Boron Nitride matrices and coatings obtained from tris (methylamino) borane. Applications to the protection of graphitic oxidation", B Bonnetot, F Guilhon, J C Viala, H Mongeot, Chem. Mater. , 299-303, (1995).

57 "Boron Nitride hard coatings by ion beam and vapor deposition", S Nishiyama, E Takahashi, Y Iwamoto, A Ebe, N Kuratani, K Ogata, Thin Solid Films, 327- 330, (1996).

58 “Formation of cubic boron nitride by the reactive sputter deposition of boron”, Alan Jankowki, Thin film solids, 94-100, (1997).

59 “Deposition of BN coatings by spraying powder accelerated electro dynamically in a coaxial pulse plasma generator” A.Olszyna, Thing film solids, 79-82, (1996).

60 “Multi layered BN coatings processed by a continuous LPCVD treatment onto Hi-Nicalon fibers”, S.Jacques, H Vincent, C Vincent, A Lopez-Marure, J Bouix, J of Solid State Chemistry, 358-363, (2001).

61 “Field emission characteristics of boron nitride films” T Sugino, Y Etou, S Tagawa, J. Vacuum Science Technology, (2000).

62 “Cubic boron nitride synthesis in low-density supersonic plasma flows” D H. Berns, M A Cappelli, Applied Physics letters, Vol 68, 2711-2713, (1996).

63 “Growth process of cubic boron nitride films in bias sputter deposition”, Y Yamada, Thin Solid Films Vol 295, 137-141, (1997).

64 “Conditions for the formation of cubic boron nitride films by r.f. magnetron sputtering” J Ye, U Rothhaar, H Oechsner, Surface and Coatings Technology Vol 105, 159-164, (1998).

65 “Preparation of cubic boron nitride films by radio frequency bias sputtering” Osamu Tsuda, Y Yamada, T Fujii, T Yoshida, J. Vacuum Science and Technology, (1995).

66 “Cubic boron nitride films grown by low energy B1 and N1 ion beam deposition” H Hofsass, Applied Physics Letters , Vol 67, 46-48, (1995).

67 “Substrate effects in cubic boron nitride film formation” P. B. Mirkarimi et al., J of Vacuum Science & Technology A: Vacuum, Surfaces, and Films ,Vol 14, 251-255, (1996).

68 “Structure and Properties of Boron Nitride Films Grown by High Temperature Reactive Plasma Deposition” S B Hyder, T O Yep, J. Electrochem. Soc., Vol 123, 1721-1724, (1976).

69 “Layered growth of boron nitride thin films” M F Plass, W Fukarek, A Kolitsch, N Schell, W Moller, Thin Solid Films, Vol 305, 172-184, (1997).

70 “CVD deposition of hexagonal BN films in reduced pressure” B Choi, Materials Research Bulletin, Vol34, 2215-2220, 1999.

71 “C60 bonding to graphite and boron nitride surfaces” P Reinke, H Feldermann, P Oelhafen, The Journal of Chemical Physics, Vol 19, 12547-12552, (2003).

72 “High temperature behavior of hexagonal boron nitride” M Hubacek, M Ueki, T Sato, V Brozek, Thermo-chimica Acta, 359-367, (1996).

73 “Boron nitride films prepared by MOCVD” K Nakamura, T Sasaki, J of solid state chemistry, 154,101-106, (2000).

74 “Plasma assisted chemical vapor deposition of boron nitride coatings from using BCl_3, N2, H2, Ar gas mixture” F Rossi, C Schaffnit, L Thomas, H Puppo, R Hugon, Vacuum, 169-181, (1999).

75 “A novel approach to deposition of cubic boron nitride coatings” I.Konyashin, J Loeffler, J Bill, F Aldinger, Thin solid films 308-309, 101-106, (1997).

76 “Investigation of the BN films prepared by low pressure CVD” JL Huang, C H Pan, D F Lii, Surface and coating technology 122, 166-175, (1999).

77 “Oxidation protection of graphite by BN coatings” A Nechepurenko, S Samuni, J of sold state chemistry 154,162-164, (2000).

78 “Nanowires in ancient Damascus steel”, W Kochmann, M Reibold, R Goldberg, W Hauffe, Journal of Alloys and Compounds, Vol 372, L15–L19, (2004).

79 “Instructions JSM-35CF Scanning Microscope” JOEL Ltd., Tokyo, Japan.

80 “Hand book X-ray Photoelectron Spectroscopy”, C D Wagner, Perkin-Elmer Corporation, MN, (1979).

81 “JSM-7401F Field Emission Scanning Electron Microscope operation guide”, JOEL Ltd, (2005).